Gondwana Research 20 (2011) 465–484

Contents lists available at ScienceDirect

Gondwana Research

journal homepage: www.elsevier.com/locate/gr

# Formation and Palaeozoic evolution of the Gorny-Altai–Altai-Mongolia suture zone (South Siberia): Zircon U/Pb constraints on the igneous record

S. Glorie [a,*], J. De Grave [a], M.M. Buslov [b], F.I. Zhimulev [b], A. Izmer [c], W. Vandoorne [a], A. Ryabinin [b], P. Van den haute [a], F. Vanhaecke [c], M.A. Elburg [a]

[a] MINPET Group, Dept. of Geology and Soil Science, Ghent University, 281/S8, Krijgslaan, B-9000 Ghent, Belgium
[b] Institute of Geology and Mineralogy, Siberian Branch of the RAS, 3 prosp. Akad. Koptyuga, 630090 Novosibirsk, Russia
[c] Dept. of Analytical Chemistry, Ghent University, Krijgslaan 281/S12, B-9000 Ghent, Belgium

ARTICLE INFO

*Article history:*
Received 1 December 2010
Received in revised form 3 March 2011
Accepted 3 March 2011
Available online 13 March 2011

Handling Editor: W.J. Xiao

*Keywords:*
Gorny Altai
Charysh–Terekta–Ulagan–Sayan suture
Central Asian Orogenic Belt
Zircon LA-ICP-MS U/Pb geochronology
Phanerozoic continental growth

ABSTRACT

The Altai-Sayan Fold Belt epitomises how Phanerozoic island-arc continental crust contributed to the growth of the Palaeo-Eurasian continent. Its formation is dominated by the closure of the Palaeo-Asian Ocean (PAO) when island-arc systems and Gondwana-derived terranes accreted to the Siberian margin. Relics of the PAO related tectonic units and associated granitoids occur along the ophiolitic Charysh–Terekta–Ulagan–Sayan suture (CTUSs) between Gorny-Altai and Altai-Mongolia. Zircon LA-ICP-MS U/Pb dating of this igneous record constrains the multi-stage geodynamic PAO evolution. Primitive Kuznetsk-Altai island-arc crust formed at the Siberian margin during the Ediacaran–Early Cambrian (525–555 Ma). This island-arc matured during the Middle–Late Cambrian (~510 Ma) and was consumed by PAO subduction in the Late Cambrian–Early Ordovician (480–490 Ma) forming the Siberian Early Caledonian accretion–collision belt. South of the CTUSs, granitic magmatism occurred within Gondwana-derived Altai-Mongolia during the Middle–Late Ordovician (450–470 Ma) Palaeo-Kazakhstan assembly and during a Silurian–Early Devonian (400–425 Ma) Andean-type collision. Middle–Late Devonian (360–395 Ma) granitoids were emplaced as a result of the collision of Altai-Mongolia with Siberia. During final Pangaea amalgamation, the suture was strike-slip reactivated (associated magmatism ~295 Ma). The youngest (220–255 Ma) sampled granitoids originated in an intra-plate setting.



## 1. Introduction

The Central Asian Orogenic Belt (CAOB) also known as the Altaids (Şengör et al., 1993) represents the world's largest accretionary orogen and stretches from the Tarim Basin on its southern border to the rigid Siberian craton in the north, from the Uralides in the west to the Pacific margin in the east (Fig. 1a). Its basement records an amalgamation of different tectonic units that formed and accreted in the geodynamic environment of the Palaeo-Asian Ocean (PAO) during the Late Precambrian–Palaeozoic (Buslov et al., 2001; Dobretsov et al., 2003; Khain et al., 2003). During this process of crustal growth, a voluminous amount of juvenile continental crust was added to the Siberian continent (Jahn et al., 2000; Buslov et al., 2002; Kovalenko et al., 2004; Kruk et al., 2010). Generally, subduction-zone magmatism is thought to be a major process in the formation of juvenile continental crust. However, it has been suggested recently that during continental growth a considerable amount of crustal material must have also been tectonically eroded by the subduction process (Yamamoto et al., 2009). Therefore, it is thought that crustal reworking has dominated crustal growth processes over juvenile additions, at least since the end of the Archean (Belousova et al., 2010). The detrital zircon record of Siberia's largest rivers confirms that recycled crust contributed to the CAOB continental growth (Safonova et al., 2010).

The Altai-Sayan Fold Belt (ASFB) or Altai-Sayan Folded Area (Sennikov et al., 2004; Dobretsov and Buslov, 2007) forms the north-western part of the CAOB and is situated between the Siberian craton and the Kazakhstan microcontinent (Fig. 1a). It extends across the political boundary zone of Russia, Kazakhstan, Kyrgyzstan, China and Mongolia. In this fold belt, no major 'mature' crustal protoliths or indicators for ancient crust have been found (Sun et al., 2008; Kruk et al., 2010). The juvenile continental crust was formed during the Late Precambrian–Early Palaeozoic evolution of island-arc systems in an open ocean or bordering a marginal basin similar to the modern analogue of South-West Japan at the Western Pacific active margin (Isozaki et al., 2010). Therefore, the ASFB epitomises a key-example of a subduction-related accretionary orogen, that is of quintessential importance in the understanding of continental growth (Buslov and Watanabe, 1996; Ota et al., 2007; Windley et al., 2007).

The intrusive record of the ASFB, i.e. the subduction-related granitoids (tonalite–granodiorite) and gabbroids that formed during

* Corresponding author. Fax: +32 9 264 4984.
*E-mail address:* Stijn.Glorie@Ugent.be (S. Glorie).

1342-937X/$ – see front matter © 2011 International Association for Gondwana Research. Published by Elsevier B.V. All rights reserved.
doi:10.1016/j.gr.2011.03.003

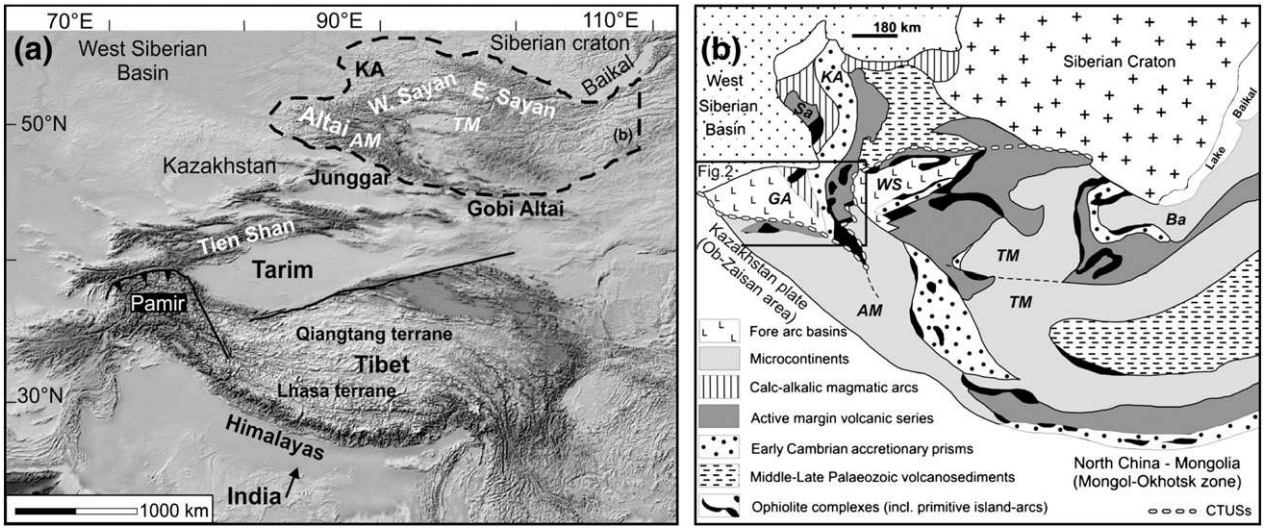


**Fig. 1.** (a) General location of the Altai-Sayan Fold Belt (ASFB) (contoured by dashed line) in the Central Asian Orogenic Belt (CAOB). (b) Simplified geological map of the ASFB, showing its main terrane subdivision: AM, Altai-Mongolia; Ba, Barguzin; GA, Gorny Altai; KA, Kuznetsk-Alatau; Sa, Salair; TM, Tuva–Mongolia; WS, West-Sayan (after Dobretsov and Buslov, 2007; De Grave et al., 2009).

the formation of the juvenile arc-continental crust on one hand and the syn- and post-collisional granitoids that formed during and after subduction–accretion of island-arcs to Siberia on the other, holds key information on the timing of accretion events and is still poorly studied. Especially absolute geochronological information is scarce and the few age data are often ambiguous in this region, resulting in conflicting interpretations when comparing different geological maps. Therefore, we performed a U/Pb geochronological study to enhance our understanding of when the island-arc continental crust was formed and added to the Siberian continent, how the different tectonic units of the ASFB are related and when they amalgamated in the CAOB.

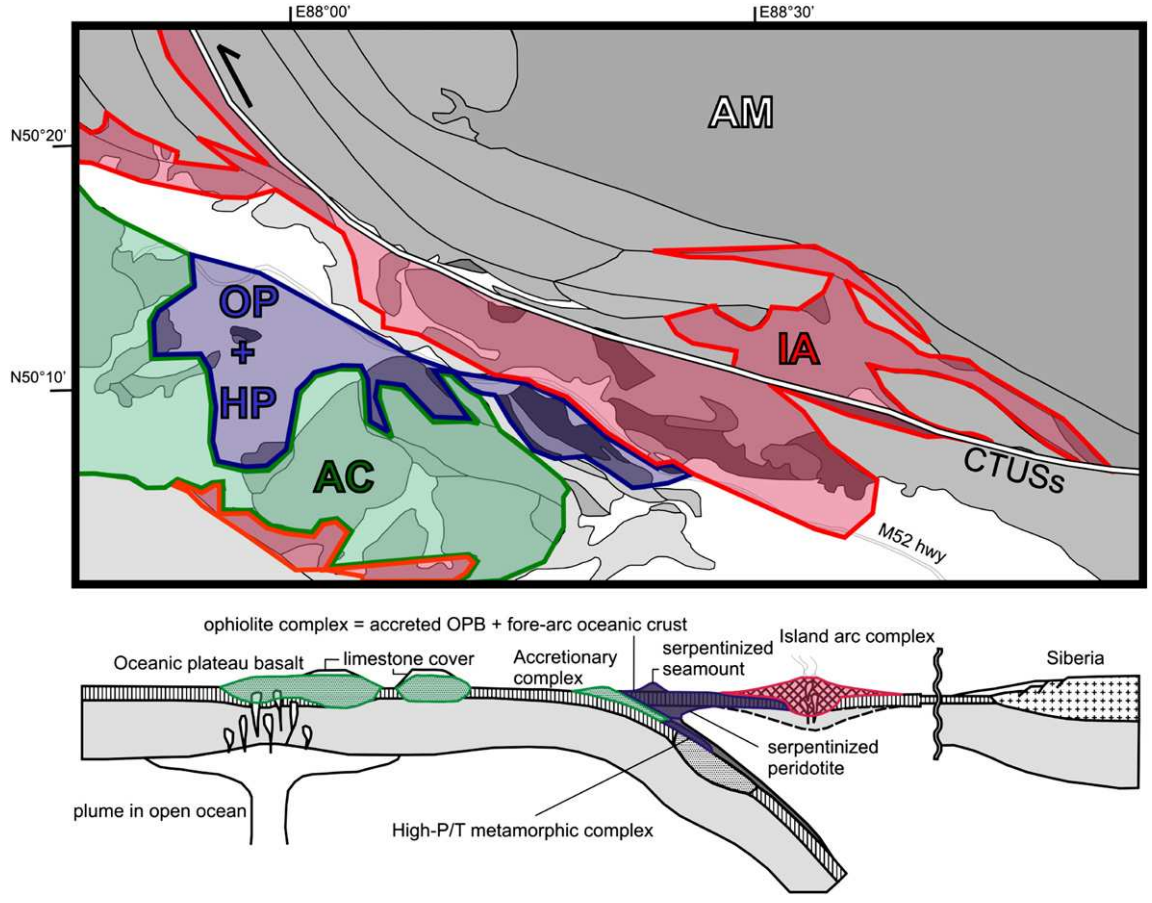


**Fig. 2.** Illustration of the evolution of the Kuznetsk-Altai island-arc system (see text for explanation). AM = Altai-Mongolia; IA = primitive Kuznetsk-Altai island-arc; OP = ophiolites; HP = High-Pressure/Temperature metamorphosed complex; AC = accretionary complex (after Ota et al., 2007).

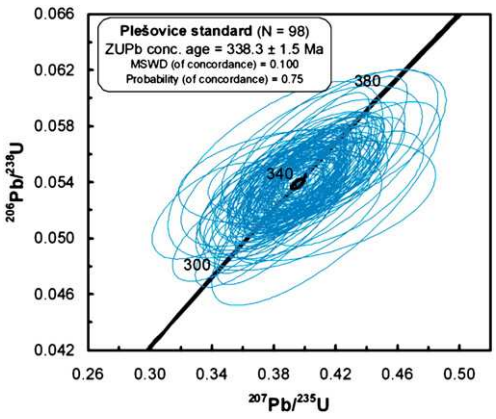


**Fig. 3.** $^{206}Pb/^{238}U$ versus $^{207}Pb/^{235}U$ concordia plot for the Plešovice zircon reference material (drawn with Isoplot; Ludwig, 2003). This secondary standard was measured repeatedly (98 analyses) through all sequences. The obtained long-term mean concordia age yields 338.3 ± 1.5 Ma, which is within error identical with the reported ID-TIMS age of 337.1 ± 0.4 Ma (Sláma et al., 2008).

## 2. Tectonic history of the Altai-Sayan Fold Belt

Located in the western part of the ASFB, Gorny Altai (GA) forms a triangle-shaped tectonic unit that is fault-bounded by a suture zone. This so-called Charysh–Terekta–Ulagan–Sayan suture-shear zone (CTUSs) (Dobretsov and Buslov, 2007; Buslov, 2011) separates Gorny Altai from its neighbouring orogenic units: West-Sayan to the east and the supposedly Gondwana-derived Altai-Mongolia (AM) terrane to the south (Fig. 1b). Following Dobretsov and Buslov (2007), the CTUSs effectively subdivides the ASFB into two segments, which both represent distinct island-arc systems that docked with the Siberian continent during the progressive closure of the PAO. In contrast to the southern segment, no Gondwana-derived microcontinents are found in the northern segment and therefore, the CTUSs represents the boundary between the Siberian marginal units in the north and the so-called Kazakhstan-Baikal composite continent in the south (present day co-ordinates) (Dobretsov and Buslov, 2007; Buslov, 2011).

The Gorny Altai terrane belongs to the northern segment. Its tectonic structure can be interpreted in the geodynamic context of accretion of the Kuznetsk-Altai island-arc system to Siberia (Fig. 1). This intra-oceanic island-arc is thought to have formed in an Ediacaran–Early Cambrian transient setting from a transform fault zone into an incipient subduction zone, close to the Siberian margin (Ota et al., 2007). During this first stage of PAO subduction, oceanic plateau basalts and seamounts arrived at the Kuznetsk-Altai arc-trench system (Buslov et al., 2002; Safonova et al., 2004, 2008, 2009). While the major part of the plateaus was subducted under the island-arc via tectonic erosion, its surficial parts accreted to form the Pacific-

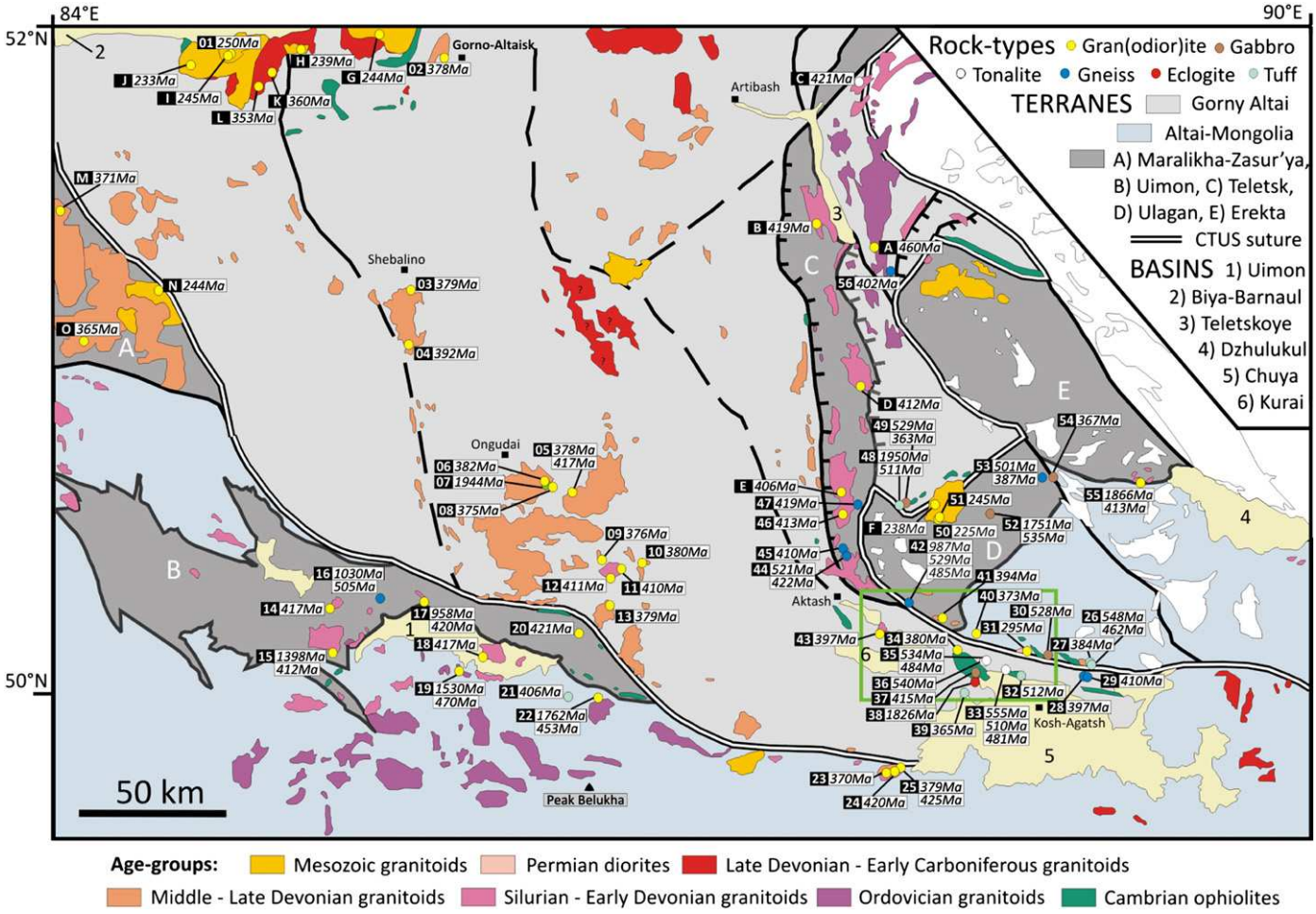


**Fig. 4.** Schematic geological map of the Charysh–Terekta–Ulagan–Sayan suture zone (CTUSs) and the neighbouring Gorny-Altai (GA) and Altai-Mongolia (AM) tectonic units, with emphasis on the magmatic record (based on Avrov, 1978; Buslov et al., 2004). All plutons are colour-coded according to their zircon U/Pb ages. The ages of the magmatic bodies in the east are uncertain and therefore, these are shown in white. Sample positions are located by dots, with a colour reference to their lithology. Zircon U/Pb concordia ages are given. Ages with a numerical prefix were obtained in this study, and for the samples with an alphabetical prefix the corresponding data were found in literature (D–F, K–O, Vladimirov et al., 2001 and references therein; G–J, Dobretsov, 2005; A–C, De Grave et al., 2009).

**Table 1**
LA-ICP-MS U/Pb results for this study. For each parameter, the arithmetic mean was calculated. A more detailed table is provided in Appendix 3.

| No. | Name | $^{207}Pb$[a] (cps) | U[b] (ppm) | Pb[b] (ppm) | Th[b] U | $^{206}Pb$ $^{204}Pb$ | $^{206}Pb$[c] $^{238}U$ | ±2s (%) | $^{207}Pb$[c] $^{235}U$ | ±2s (%) | $^{207}Pb$[c] $^{206}Pb$ | ±2s (%) | rho[d] | $^{206}Pb$[e] $^{238}U$ | ±2s (Ma) | $^{207}Pb$[e] $^{235}U$ | ±2s (Ma) | con.[f] | N[g] | conc. Age[h] (Ma) | Note[i] | Group |
|---|---|---|---|---|---|---|---|---|---|---|---|---|---|---|---|---|---|---|---|---|---|---|
| 1 | Be-01 | 1166 | 333 | 14 | 0.45 | 1341 | 0.0393 | 7.9 | 0.2916 | 16 | 0.0538 | 14 | 0.51 | 248 | 19 | 260 | 38 | 105 | 14 | 250 ± 6 | Concordant | VIII |
| 2 | GA-01 | 762 | 186 | 11 | 0.16 | 1189 | 0.0604 | 7.7 | 0.4613 | 15 | 0.0554 | 13 | 0.52 | 378 | 28 | 385 | 49 | 102 | 19 | 378 ± 6 | Concordant | I |
| 3 | KU-01 | 2654 | 923 | 57 | 0.29 | 6999 | 0.0607 | 5.4 | 0.4570 | 9.2 | 0.0573 | 7.3 | 0.62 | 380 | 20 | 382 | 30 | 101 | 12 | 379 ± 6 | Concordant | I |
| 4 | KU-05 | 2820 | 284 | 18 | 0.30 | 6203 | 0.0627 | 4.5 | 0.4901 | 7.9 | 0.0568 | 6.5 | 0.57 | 392 | 17 | 405 | 27 | 103 | 9 | 392 ± 8 | Concordant | I |
| 5 | KU-29 | 1281 | 257 | 16 | 0.28 | 3319 | 0.0602 | 4.6 | 0.4696 | 10 | 0.0566 | 9.2 | 0.47 | 377 | 17 | 391 | 35 | 104 | 12 | 378 ± 7 | Concordant comp. 1 | I |
| | | 1855 | 326 | 24 | 0.60 | 5321 | 0.0667 | 4.3 | 0.5074 | 8.0 | 0.0552 | 6.7 | 0.54 | 416 | 17 | 416 | 27 | 100 | 3 | 417 ± 10 | Concordant comp. 2 | |
| 6 | KU-08 | 672 | 110 | 7 | 0.39 | 1385 | 0.0612 | 4.3 | 0.4584 | 12 | 0.0543 | 11 | 0.38 | 383 | 16 | 383 | 39 | 100 | 22 | 382 ± 4 | Concordant | I |
| 7 | KU-07 | 16734 | 621 | 178 | 0.27 | 6348 | 0.3051 | 5.9 | 4.9241 | 8.3 | 0.1224 | 5.4 | 0.69 | 1715 | 86 | 1799 | 72 | 105 | 7 | 1944 ± 44 | Upper-intcpt. | VII |
| 8 | KU-86 | 258 | 54 | 3 | 0.33 | 212 | 0.0587 | 8.9 | 0.4441 | 50 | 0.0548 | 49 | 0.23 | 368 | 31 | 369 | 155 | 100 | 10 | 375 ± 10 | Concordant | I |
| 9 | KU-26 | 543 | 129 | 8 | 0.33 | 691 | 0.0611 | 7.2 | 0.4988 | 21 | 0.0590 | 19 | 0.36 | 382 | 27 | 390 | 65 | 103 | 8 | 376 ± 14 | Concordant | I |
| 10 | KU-35 | 401 | 216 | 13 | 0.32 | 873 | 0.0611 | 5.9 | 0.4740 | 20 | 0.0563 | 19 | 0.32 | 382 | 22 | 394 | 69 | 103 | 14 | 380 ± 6 | Concordant | I |
| 11 | KU-34 | 1787 | 220 | 16 | 0.48 | 1206 | 0.0659 | 4.0 | 0.5120 | 8.6 | 0.0554 | 6.9 | 0.51 | 411 | 16 | 420 | 30 | 102 | 10 | 410 ± 7 | Concordant | II |
| 12 | KU-16 | 1023 | 182 | 13 | 0.59 | 3058 | 0.0658 | 5.5 | 0.5033 | 14 | 0.0555 | 13 | 0.43 | 411 | 22 | 414 | 48 | 101 | 20 | 411 ± 5 | Concordant | II |
| 13 | KU-10 | 1198 | 207 | 13 | 0.37 | 3948 | 0.0607 | 4.7 | 0.4617 | 12 | 0.0552 | 11 | 0.49 | 380 | 17 | 385 | 39 | 101 | 12 | 379 ± 4 | Concordant | I |
| 14 | B-09-03 | 3116 | 484 | 32 | 0.29 | 4809 | 0.0660 | 7.6 | 0.4896 | 14 | 0.0592 | 12 | 0.53 | 412 | 30 | 404 | 48 | 98 | 16 | 417 ± 7 | Concordant | II |
| 15 | B-09-20 | 4972 | 1496 | 100 | 0.39 | 6001 | 0.0660 | 5.0 | 0.4434 | 7.9 | 0.0512 | 6.1 | 0.64 | 412 | 20 | 373 | 25 | 90 | 3 | 412 ± 22 | $^{206}Pb/^{238}U$ mean age | II |
| | | 35971 | 1438 | 372 | 0.37 | 27096 | 0.2453 | 5.9 | 2.9876 | 8.3 | 0.0924 | 5.8 | 0.71 | 1413 | 74 | 1399 | 65 | 99 | 4 | 1398 ± 76 | Upper-intcpt. | |
| 16 | D-01-10 | 1276 | 119 | 11 | 0.37 | 1683 | 0.0810 | 8.2 | 0.6588 | 22 | 0.0591 | 20 | 0.46 | 502 | 39 | 514 | 92 | 102 | 8 | 505 ± 13 | Concordant comp. 1 | IV |
| | | 1511 | 81 | 11 | 0.46 | 1880 | 0.1310 | 5.2 | 1.2821 | 9.6 | 0.0704 | 8.0 | 0.55 | 792 | 39 | 830 | 55 | 105 | 4 | 1030 ± 170 | Upper-intcpt. comp. 2 | |
| 17 | D-01-07 | 1301 | 175 | 12 | 0.26 | 2801 | 0.0666 | 7.0 | 0.5335 | 16 | 0.0581 | 14 | 0.50 | 416 | 28 | 434 | 60 | 104 | 15 | 420 ± 6 | Concordant comp. 1 | II |
| | | 6759 | 361 | 50 | 0.24 | 3388 | 0.1362 | 4.2 | 1.2881 | 6.5 | 0.0684 | 4.9 | 0.65 | 822 | 33 | 837 | 38 | 102 | 2 | 958 ± 120 | Upper-intcpt. comp. 2 | |
| 18 | B-09-49 | 1504 | 166 | 12 | 0.47 | 1257 | 0.0670 | 7.7 | 0.5044 | 23 | 0.0601 | 21 | 0.36 | 418 | 31 | 413 | 81 | 99 | 14 | 417 ± 10 | Concordant | II |
| 19 | B-09-43 | 2014 | 358 | 31 | 0.56 | 1248 | 0.0784 | 14 | 0.6249 | 27 | 0.0575 | 22 | 0.58 | 486 | 48 | 491 | 88 | 101 | 11 | 470 ± 18 | Concordant comp. 1 | III |
| | | 5114 | 127 | 40 | 0.42 | 1678 | 0.2911 | 19 | 3.8722 | 22 | 0.0964 | 11 | 0.82 | 1646 | 199 | 1604 | 141 | 98 | 2 | 1530 ± 69 | Upper-intcpt. comp. 2 | |
| 20 | KU-39 | 7726 | 984 | 70 | 0.54 | 2773 | 0.0686 | 6.0 | 0.6798 | 9.8 | 0.0710 | 7.6 | 0.65 | 428 | 25 | 515 | 43 | 119 | 14 | 421 ± 7 | Lower-intcpt | II |
| 21 | D-07-02 | 2036 | 298 | 20 | 0.25 | 5410 | 0.0654 | 4.8 | 0.4903 | 9.3 | 0.0543 | 7.8 | 0.53 | 409 | 19 | 405 | 32 | 99 | 22 | 406 ± 3 | Concordant | II |
| 22 | B-09-60 | 1602 | 173 | 14 | 0.60 | 515 | 0.0731 | 2.8 | 0.5928 | 7.9 | 0.0588 | 7.4 | 0.35 | 455 | 12 | 473 | 30 | 104 | 3 | 453 ± 7 | Concordant comp. 1 | III |
| | | 3477 | 57 | 17 | 0.46 | 4539 | 0.2361 | 6.5 | 3.4494 | 11 | 0.1058 | 8.5 | 0.64 | 1359 | 77 | 1492 | 87 | 113 | 9 | 1762 ± 80 | Upper-intcpt. comp. 2 | |
| 23 | G-07-02 | 2263 | 343 | 21 | 0.56 | 5400 | 0.0575 | 13 | 0.4575 | 16 | 0.0577 | 9.1 | 0.78 | 361 | 44 | 382 | 52 | 106 | 7 | 370 ± 19 | Concordant | I |
| 24 | G-07-04 | 1498 | 248 | 19 | 0.70 | 1155 | 0.0670 | 5.1 | 0.5264 | 9.8 | 0.0571 | 8.2 | 0.53 | 418 | 21 | 429 | 35 | 103 | 5 | 420 ± 8 | Concordant | II |
| 25 | G-07-07 | 767 | 182 | 12 | 0.50 | 1510 | 0.0613 | 6.5 | 0.4363 | 16 | 0.0516 | 14 | 0.43 | 384 | 25 | 367 | 50 | 96 | 14 | 379 ± 6 | Concordant comp. 1 | I |
| | | 1135 | 249 | 19 | 0.61 | 1762 | 0.0680 | 10 | 0.5338 | 19 | 0.0570 | 16 | 0.52 | 424 | 41 | 434 | 72 | 102 | 7 | 425 ± 12 | Concordant comp. 2 | |
| 26 | KU-52 | 2385 | 348 | 25 | 0.22 | 3300 | 0.0737 | 6.0 | 0.5808 | 10 | 0.0571 | 8.0 | 0.60 | 459 | 27 | 465 | 38 | 101 | 11 | 462 ± 8 | Concordant comp. 1 | |
| | | 4440 | 544 | 48 | 0.25 | 2872 | 0.0896 | 7.3 | 0.7346 | 10 | 0.0595 | 6.5 | 0.70 | 553 | 39 | 559 | 44 | 101 | 4 | 548 ± 15 | Concordant comp. 2 | VI |
| 27 | KU-57 | 2970 | 519 | 34 | 0.35 | 14991 | 0.0616 | 6.8 | 0.4783 | 11 | 0.0564 | 8.2 | 0.65 | 385 | 25 | 397 | 36 | 103 | 13 | 384 ± 9 | Concordant | I |
| 28 | B-09-79 | 1188 | 221 | 15 | 0.52 | 1402 | 0.0630 | 5.6 | 0.4843 | 12 | 0.0558 | 9.9 | 0.50 | 394 | 21 | 401 | 39 | 102 | 15 | 397 ± 5 | Concordant | II |
| 30 | F-09327 | 1597 | 182 | 17 | 0.35 | 6220 | 0.0859 | 7.2 | 0.7012 | 14 | 0.0592 | 12 | 0.56 | 531 | 37 | 539 | 62 | 101 | 12 | 528 ± 10 | Concordant | VI |
| 31 | 07-26 | 86 | 20 | 1 | 0.18 | 158 | 0.0465 | 8.1 | 0.3547 | 38 | 0.0554 | 37 | 0.22 | 293 | 23 | 308 | 106 | 105 | 10 | 295 ± 6 | Concordant comp. 1 | VIII |
| | | 431 | 61 | 3 | 0.18 | 2770 | 0.0564 | 10 | 0.4647 | 20 | 0.0599 | 18 | 0.50 | 354 | 36 | 387 | 68 | 110 | 5 | 355 ± 21 | Concordant comp. 2 | |
| 32 | KU-51 | 6078 | 896 | 72 | 0.18 | 14545 | 0.0817 | 6.7 | 0.6580 | 8.0 | 0.0584 | 4.1 | 0.81 | 506 | 33 | 513 | 33 | 101 | 21 | 512 ± 7 | Concordant | V |

| No. | Name | $^{207}Pb$[a] (cps) | U[b] (ppm) | Pb[b] (ppm) | Th[b] U | $^{206}Pb$ $^{204}Pb$ | $^{206}Pb$[c] $^{238}U$ | ±2s (%) | $^{207}Pb$[c] $^{235}U$ | ±2s (%) | $^{207}Pb$[c] $^{206}Pb$ | ±2s (%) | rho[d] | $^{206}Pb$[e] $^{238}U$ | ±2s (Ma) | $^{207}Pb$[e] $^{235}U$ | ±2s (Ma) | con.[f] | N[g] | conc. Age[h] (Ma) | Note[i] | Group |
|---|---|---|---|---|---|---|---|---|---|---|---|---|---|---|---|---|---|---|---|---|---|---|
| 33 | KU-43 | 971 | 75 | 6 | 0.18 | 326 | 0.0775 | 3.5 | 0.5900 | 13 | 0.0552 | 12 | 0.31 | 481 | 16 | 471 | 48 | 98 | 2 | 481 ± 11 | Concordant comp. 1 | |
| | | 1084 | 75 | 6 | 0.18 | 1258 | 0.0829 | 4.3 | 0.6900 | 12 | 0.0604 | 11 | 0.43 | 514 | 22 | 533 | 52 | 104 | 8 | 510 ± 11 | Concordant comp. 2 | |
| | | 487 | 32 | 3 | 0.19 | 363 | 0.0905 | 4.6 | 0.7358 | 17 | 0.0590 | 16 | 0.29 | 559 | 24 | 559 | 74 | 100 | 6 | 555 ± 10 | Concordant comp. 3 | VI |
| 34 | KU-67 | 1993 | 493 | 31 | 0.38 | 5800 | 0.0605 | 5.7 | 0.4641 | 8.8 | 0.0556 | 6.5 | 0.66 | 379 | 21 | 387 | 29 | 102 | 9 | 380 ± 10 | Concordant | I |
| 35 | 07-28 | 2717 | 266 | 22 | 0.60 | 2941 | 0.0768 | 8.2 | 0.6206 | 13 | 0.0585 | 9.8 | 0.61 | 477 | 38 | 490 | 52 | 103 | 3 | 484 ± 13 | Concordant comp. 1 | |
| | | 7513 | 663 | 72 | 0.93 | 4355 | 0.0866 | 4.9 | 0.7115 | 7.8 | 0.0596 | 5.8 | 0.65 | 535 | 25 | 545 | 34 | 102 | 13 | 534 ± 8 | Concordant comp. 2 | VI |
| 36 | 07-29 | 2169 | 230 | 20 | 0.15 | 3388 | 0.0877 | 5.2 | 0.7159 | 9.7 | 0.0592 | 8.1 | 0.55 | 542 | 27 | 548 | 42 | 101 | 18 | 540 ± 8 | Concordant | VI |
| 37 | KU-48 | 9955 | 818 | 102 | 0.34 | 1487 | 0.0662 | 3.5 | 0.4877 | 7.5 | 0.2680 | 6.6 | 0.47 | 413 | 14 | 403 | 25 | 98 | 2 | 415 ± 10 | Concordant | II |
| 38 | B-09-90 | 99854 | 1380 | 434 | 0.05 | 23838 | 0.3224 | 4.7 | 5.0114 | 5.3 | 0.1128 | 2.5 | 0.88 | 1801 | 74 | 1821 | 46 | 101 | 2 | 1826 ± 27 | Concordant | VII |
| 39 | KU-50b | 1946 | 461 | 27 | 0.34 | 2711 | 0.0583 | 7.0 | 0.4505 | 11 | 0.0561 | 7.7 | 0.67 | 365 | 25 | 378 | 34 | 104 | 11 | 365 ± 10 | Concordant | I |
| 40 | KU-84 | 3359 | 926 | 53 | 0.24 | 5117 | 0.0588 | 9.2 | 0.4436 | 11 | 0.0547 | 5.5 | 0.77 | 369 | 33 | 373 | 36 | 101 | 13 | 373 ± 8 | Concordant | I |
| 41 | AL-240 | 1929 | 380 | 25 | 0.36 | 12782 | 0.0626 | 9.8 | 0.4920 | 14 | 0.0570 | 8.9 | 0.71 | 392 | 37 | 406 | 47 | 104 | 10 | 394 ± 9 | Concordant | II |
| 42 | D-01-15 | 2728 | 335 | 27 | 0.37 | 2437 | 0.0779 | 6.3 | 0.6158 | 11 | 0.0573 | 9.0 | 0.57 | 484 | 29 | 487 | 44 | 101 | 6 | 485 ± 10 | Concordant comp. 1 | |
| | | 4434 | 516 | 43 | 0.17 | 25565 | 0.0851 | 6.4 | 0.6710 | 8.2 | 0.0571 | 5.1 | 0.78 | 527 | 33 | 521 | 34 | 99 | 3 | 529 ± 18 | Concordant comp. 2 | VI |
| | | 8230 | 405 | 68 | 0.35 | 3204 | 0.1632 | 5.6 | 1.6156 | 7.3 | 0.0717 | 4.5 | 0.75 | 974 | 52 | 975 | 47 | 100 | 5 | 987 ± 21 | Concordant comp. 3 | |
| 43 | KU-59 | 1504 | 191 | 12 | 0.22 | 1771 | 0.0644 | 5.7 | 0.4881 | 9.9 | 0.0550 | 8.1 | 0.58 | 399 | 22 | 403 | 34 | 100 | 17 | 397 ± 5 | Concordant | II |
| 44 | KU-42 | 7336 | 1221 | 76 | 0.02 | 10808 | 0.0672 | 7.1 | 0.5254 | 9.9 | 0.0568 | 6.8 | 0.71 | 419 | 29 | 429 | 35 | 102 | 13 | 422 ± 7 | Concordant comp. 1 | II |
| | | 2700 | 345 | 30 | 0.37 | 6827 | 0.0841 | 5.1 | 0.6840 | 8.1 | 0.0590 | 6.2 | 0.65 | 520 | 26 | 529 | 34 | 102 | 2 | 521 ± 18 | Concordant comp. 2 | |
| 45 | KU-41 | 3573 | 1122 | 72 | 0.19 | 17058 | 0.0653 | 5.5 | 0.5264 | 9.6 | 0.0585 | 7.8 | 0.58 | 408 | 22 | 429 | 34 | 105 | 6 | 410 ± 13 | Concordant | II |
| 46 | KU-71 | 2008 | 430 | 31 | 0.55 | 1352 | 0.0662 | 5.9 | 0.5155 | 9.9 | 0.0564 | 7.8 | 0.61 | 413 | 24 | 422 | 35 | 102 | 17 | 413 ± 5 | Concordant | II |
| 47 | KU-68 | 2432 | 316 | 22 | 0.34 | 2904 | 0.0678 | 4.4 | 0.5071 | 7.5 | 0.0542 | 6.0 | 0.59 | 423 | 18 | 416 | 26 | 98 | 16 | 419 ± 4 | Concordant | II |
| 48 | KU-83 | 3340 | 167 | 18 | 0.40 | 2736 | 0.0822 | 8.5 | 0.6685 | 16 | 0.0521 | 15 | 0.60 | 509 | 42 | 520 | 67 | 102 | 10 | 511 ± 12 | Concordant comp. 1 | V |
| | | 14535 | 83 | 36 | 0.41 | 17473 | 0.3424 | 7.9 | 5.5814 | 11 | 0.1040 | 7.9 | 0.73 | 1897 | 130 | 1907 | 95 | 100 | 3 | 1950 ± 85 | Upper-intcpt. comp. 2 | |
| 49 | KU-82 | 790 | 64 | 4 | 0.23 | 1948 | 0.0589 | 9.7 | 0.4626 | 23 | 0.0567 | 20 | 0.46 | 369 | 35 | 385 | 75 | 104 | 5 | 363 ± 14 | Concordant | |
| | | 1343 | 66 | 6 | 0.33 | 1540 | 0.0854 | 9.5 | 0.7483 | 22 | 0.0637 | 20 | 0.48 | 528 | 48 | 567 | 104 | 108 | 11 | 529 ± 13 | Concordant | VI |
| 50 | KU-79 | 2192 | 305 | 13 | 0.45 | 1483 | 0.0355 | 8.8 | 0.2626 | 13 | 0.0498 | 11 | 0.68 | 225 | 19 | 237 | 28 | 105 | 16 | 225 ± 5 | Concordant | VIII |
| 51 | KU-78b | 1133 | 533 | 23 | 0.51 | 2113 | 0.0386 | 5.3 | 0.2902 | 12 | 0.0546 | 11 | 0.46 | 244 | 13 | 259 | 29 | 106 | 12 | 245 ± 5 | Concordant | VIII |
| 52 | GA-21 | 265 | 25 | 2 | 0.36 | 179 | 0.0876 | 11 | 0.8905 | 45 | 0.0744 | 43 | 0.28 | 542 | 58 | 643 | 248 | 120 | 11 | 535 ± 16 | Concordant comp. 1 | VI |
| | | 437 | 6 | 3 | 1.41 | 464 | 0.3705 | 13 | 5.2539 | 42 | 0.1019 | 40 | 0.33 | 2031 | 233 | 1842 | 453 | 90 | 2 | 1751 ± 450 | Upper-intcpt. comp. 2 | |
| 53 | GA-18 | 1372 | 131 | 9 | 0.18 | 475 | 0.0656 | 12 | 0.4931 | 25 | 0.0544 | 21 | 0.52 | 410 | 47 | 406 | 84 | 99 | 2 | 387 ± 30 | Concordant comp. 1 | |
| | | 4466 | 362 | 30 | 0.29 | 1824 | 0.0806 | 9.1 | 0.6212 | 13 | 0.0559 | 8.4 | 0.73 | 500 | 44 | 490 | 51 | 98 | 7 | 501 ± 15 | Concordant comp. 2 | IV |
| 54 | GA-07 | 11211 | 1718 | 139 | 1.06 | 47221 | 0.0584 | 9.7 | 0.4395 | 11 | 0.0546 | 5.0 | 0.87 | 366 | 35 | 370 | 35 | 101 | 11 | 367 ± 9 | Concordant | I |
| 55 | GA-20 | 2481 | 300 | 20 | 0.21 | 1497 | 0.0682 | 4.9 | 0.5213 | 8.2 | 0.0554 | 6.2 | 0.59 | 425 | 21 | 426 | 29 | 100 | 3 | 413 ± 8 | Concordant comp. 1 | II |
| | | 21088 | 260 | 94 | 0.38 | 11059 | 0.3372 | 4.0 | 5.2768 | 5.3 | 0.1135 | 3.3 | 0.74 | 1873 | 65 | 1865 | 46 | 100 | 9 | 1866 ± 14 | Concordant comp. 2 | |
| 56 | SH-18 | 6747 | 682 | 43 | 0.19 | 27965 | 0.0649 | 6.6 | 0.4885 | 10 | 0.0546 | 7.1 | 0.71 | 405 | 26 | 404 | 34 | 100 | 15 | 402 ± 6 | Concordant | II |

[a] Within-run, background-corrected mean $^{207}Pb$ signal.
[b] U and Pb content and Th/U ratio were calculated relative to the GJ-1 zircon standard.
[c] Corrected for: background, within-run Pb/U fractionation ($^{206}Pb/^{238}U$), where needed common Pb (Stacey and Kramers, 1975) and subsequently normalised to GJ-1 (Instrumental drift corrected).
[d] rho is the error correlation defined as $err^{206}Pb/^{238}U/err^{207}Pb/^{235}U$.
[e] U/Pb ages were calculated with Isoplot (Ludwig, 2003).
[f] Degree of concordance = $age^{206}Pb/^{238}U/age^{207}Pb/^{206}Pb \times 100$.
[g] Number of targets (some grains yielded 2 targets).
[h] Concordant or Intercept age as calculated with Isoplot (Ludwig, 2003). Concordia plots are shown in Fig. 5.
[i] Some samples yielded several concordant components or a lower/upper intercept with the concordia curve.

type Gorny-Altai accretionary complex. Remnants of these seamounts and oceanic plateaus are found in the OP (ophiolitic) and HP (High-Pressure/Temperature metamorphosed) complex bordering the island-arc magmatic rocks (Fig. 2). During the Middle–Late Cambrian, the Kuznetsk-Altai island-arc had evolved into a mature stage, characterised by calc-alkaline volcanism. It accreted onto the Siberian continent in the Late Cambrian–Early Ordovician (Buslov et al., 2002, 2004; Dobretsov and Buslov, 2007; Ota et al., 2007; Safonova et al., 2008, 2009).

The current western section of the Kazakhstan-Baikal composite continent (Dobretsov and Buslov, 2007) corresponds to the Kazakhstan microcontinent or Palaeo-Kazakhstan, defined by Windley et al. (2007). This tectonic unit is composed of Gondwana-derived terranes (including AM), which were subducted-accreted to the Kazakhstan–Tuva–Mongolian island-arc. This second island-arc system occupied a more seaward position in the PAO with respect to Siberia and the Kuznetsk-Altai island-arc, where at the end of the Ordovician, Palaeo-Kazakhstan amalgamated (Fig. 1b). AM served as a microcontinental nucleus in the Palaeo-Kazakhstan edifice, where Andean-type arcs were built along its margins during the Early Palaeozoic (Windley et al., 2002; Wang et al., 2006; Windley et al., 2007).

The collision of Palaeo-Kazakhstan with Siberia occurred in a diachronic fashion, possibly already starting in the Ordovician in the Baikal region (Fig. 1) (Dobretsov and Buslov, 2007; Buslov, 2011). Later, during the Late Devonian–Early Carboniferous, AM (as part of Palaeo-Kazakhstan) collided with the Siberian margin and the CTUSs was formed. This collision event was accompanied by the intrusion of a granitoid batholith into the Ediacaran–Early Palaeozoic accretionary complexes of Gorny Altai. At this time, only remnant oceanic tracts of the PAO remained, such as the Ob'-Zaysan Ocean, which finally closed in the Late Carboniferous–Permian, resulting in the collisions of Siberia, Baltica and Palaeo-Kazakhstan (Buslov et al., 2001; Dobretsov et al., 2004). These Late Palaeozoic collisions induced extensive strike-slip and thrust-movements, which created a typical mosaic-blocky structure that added to the complexity of the ASFB (Buslov et al., 2004; Buslov, 2011).

During the above described stages of subduction–accretion and collision of this variety of tectonic units to the Siberian margin, several plutons were emplaced in the continental crust. Their crystallisation age holds key information in understanding the several stages succeeding continental growth (Vladimirov et al., 2001; Jahn, 2004; Kruk et al., 2010).

## 3. Analytical procedures

During several field-campaigns, a large number of igneous basement samples along the CTUSs were collected. After crushing, sieving and conventional density and magnetic separation, zircon crystals were separated from a total of 56 basement samples from this sample-set. For each sample, around 40 zircon grains were selected, mounted in epoxy and polished for subsequent U/Pb dating. Prior to the U/Pb analysis, the internal structure of the zircon grains was investigated and mapped with back-scattered-electron (BSE) and cathodoluminescence (CL) imaging, using a JEOL JSM-6400 SEM (Scanning Electron Microscope). Using this technique, possible inherited cores and oscillatory magmatic zonation in the zircons were identified and a robust target selection was done. The U/Pb analyses were carried out with the LA-ICP-(SF)-MS (Laser Ablation-Inductively Coupled Plasma-Sector Field-Mass Spectrometry) facility of the Department of Analytical Chemistry, Ghent University, with analytical procedures following Glorie et al. (2010). A New Wave Research UP193HE ArF-excimer-based laser ablation system (Fremont, CA, USA) was equipped with a teardrop-shaped low-volume (<2.5 $cm^3$) ablation cell (Gerdes and Zeh, 2009; Glorie et al., 2010) and coupled to the mass spectrometer. Helium was used as carrier gas, whereby argon was introduced and admixed with the helium after the ablation cell. Determination of U(-Th)/Pb ratios was carried out using a Thermo Scientific Element XR Sector Field ICP-MS unit (Bremen, Germany; e.g. Frei and Gerdes, 2009). Instrumental details are listed in Appendix 1. A series of runs (50 unknowns, 13 primary, 5 secondary standard measurements) is defined as a sequence. Within one sequence, all runs are carried out using the same instrumental settings and data reduction is accomplished relying on the same procedure. To control this, we used an electronic trigger between the laser and the mass spectrometer that allows us to measure during the exact same time interval after laser warm-up. Data reduction was performed using the PepiAGE-software (Dunkl et al., 2009). Laser-induced elemental fractionation was corrected for by using the arithmetic mean ratio for each run. Instrumental mass discrimination was corrected for by normalisation to the reference zircon GJ-1, which was measured repeatedly during each sequence (Jackson et al., 2004). Drift correction was done by applying a best fit through the measured ratios for the GJ-1 standard. The function applied for this best fit regression-line (linear, logarithmic, second-order, third-order) varies between each sequence, depending on daily variations in instrumental conditions (Appendix 1). Resulting concordia ages were calculated with the Isoplot software (Ludwig, 2003). The Plešovice (Sláma et al., 2008) zircon standard was measured multiple times throughout each sequence and serves as an accuracy check. Our long-term (98 analyses) mean concordia age obtained for this secondary standard yields 338.3 ± 1.5 Ma, which is in good agreement with the reported ID-TIMS age of 337.1 ± 0.4 Ma (Sláma et al., 2008) (Fig. 3).

## 4. Zircon U/Pb results: Identification of age-groups

Sample locations are plotted on a simplified geological map showing the structural pattern of the study-area and the extension of the ophiolitic complexes and granitoid plutons (Fig. 4). As shown, sampling occurred mainly along the CTUSs, wedged in between GA and AM. Each intrusion is colour-coded according to the zircon U/Pb age obtained in this study or found in literature. Where no U/Pb data is available, the age of the intrusions is considered uncertain and therefore, they are shown in white. Samples with a numerical prefix on the map are dated in this study, for the samples with an alphabetical prefix information was found in literature (Vladimirov et al., 2001 and references therein; Dobretsov, 2005; De Grave et al., 2009). A description of the sample localities and lithologies is given in Appendix 2. Based on their lithology and geodynamic nature, the samples can be grouped in six different types of igneous rocks. The first and most common type of samples originate from granitoids that were emplaced during syn- and post-collisional stages of the growth of the Palaeo-Kazakhstan (in AM) and Siberian continents (in GA). Several of these intrusives underwent regional metamorphism to form gneissic terranes. These ortho-gneisses represent our second lithology type. They are mainly found in the Uimon and Teletsk units, which are thrusted and sheared allochtonous terranes along the southern and eastern margin of GA (Fig. 4). A third lithology-type consists of gabbroids and subduction-related tonalites–granodiorites that represent several formation stages of arc-continental crust. Some of their extrusive equivalents (acidic to intermediate tuffs) also yielded sufficient zircon to be used for U/Pb dating and constitute the fourth type of igneous rocks. The fifth type of samples comprises intrusives (granitoids and mafic dikes), which are considered to be emplaced in an intra-plate setting. A single sample marks the sixth rock-type, i.e. high-pressure (eclogitic) rocks in the Chagan-Uzun area (see further).

**Fig. 5.** $^{206}Pb/^{238}U$ versus $^{207}Pb/^{235}U$ concordia plots (drawn with Isoplot; Ludwig, 2003), arranged by their age from young to old, except for the Permian and Mesozoic post-collisional samples, which are located at the end of the figure. All data-point error-ellipses were calculated at 2σ-level. Where concordant ages were obtained, the central bold ellipse represents the concordia age with its uncertainty. Some samples yielded multiple concordant age-groups. For others, discordant ages arranged along a discordia-line (bold dashed line) define upper- and lower-intercept ages with concordia. The numbers in italic refer to the sample positions in Fig. 4.

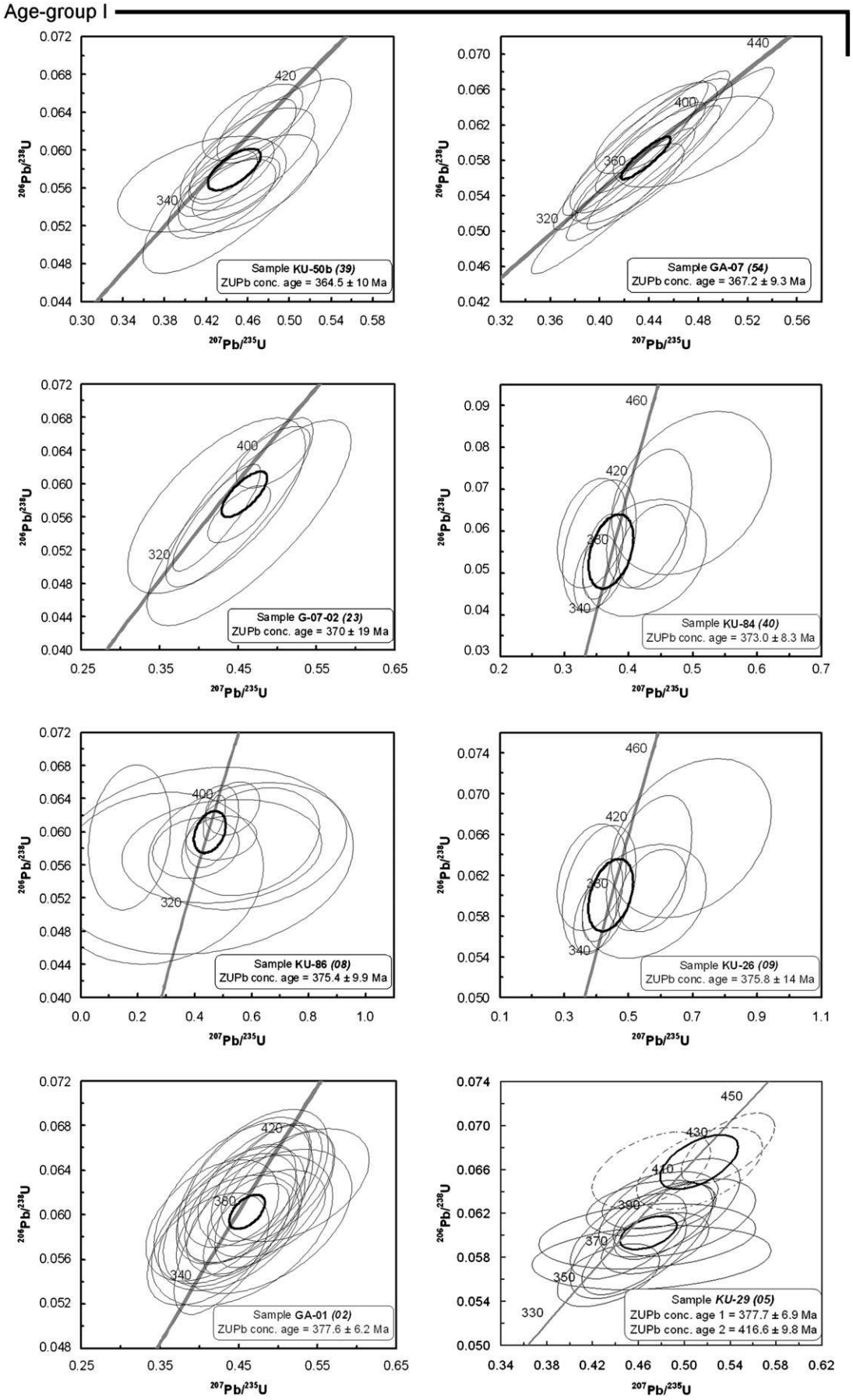

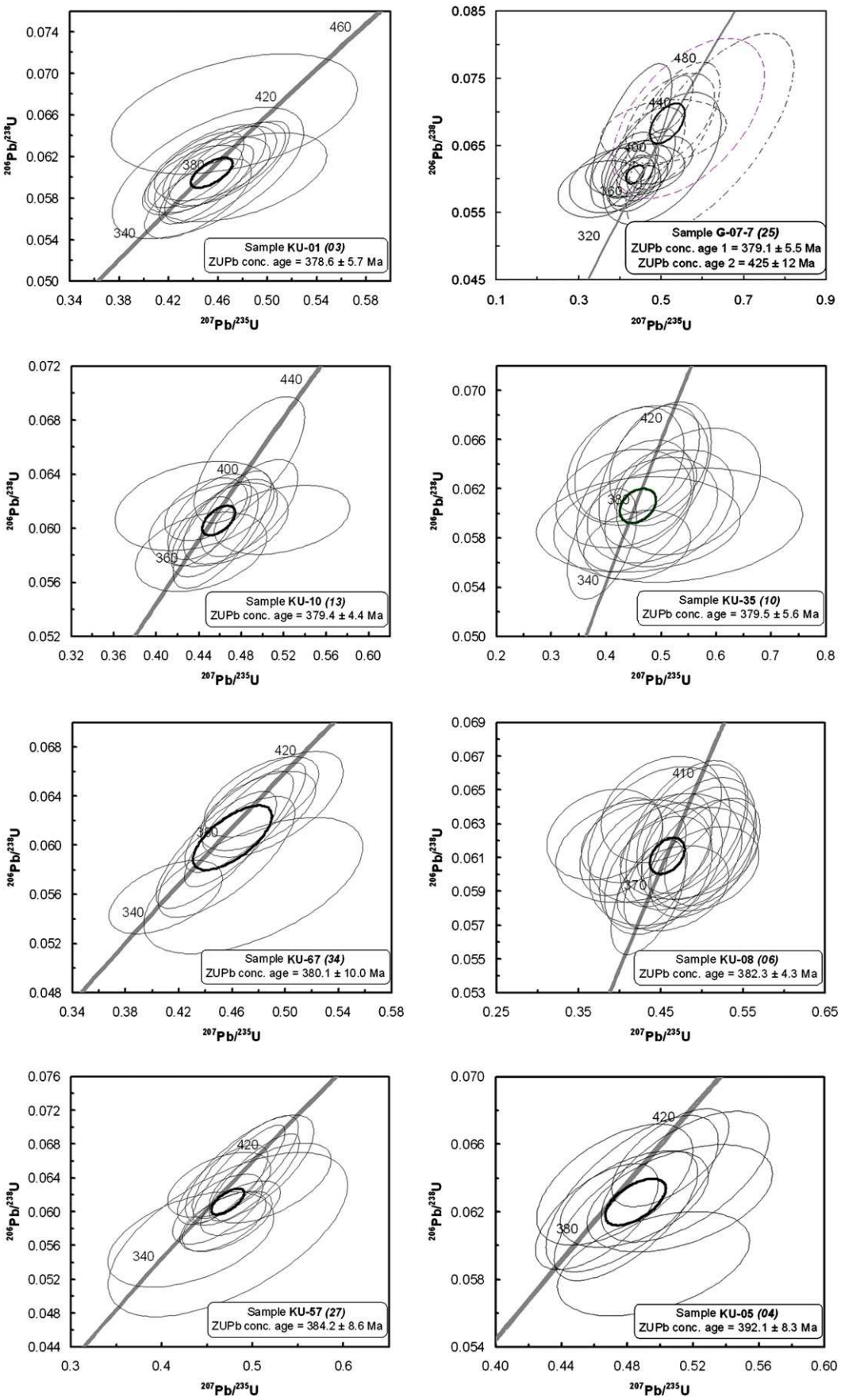


**Fig. 5.** (*continued*).

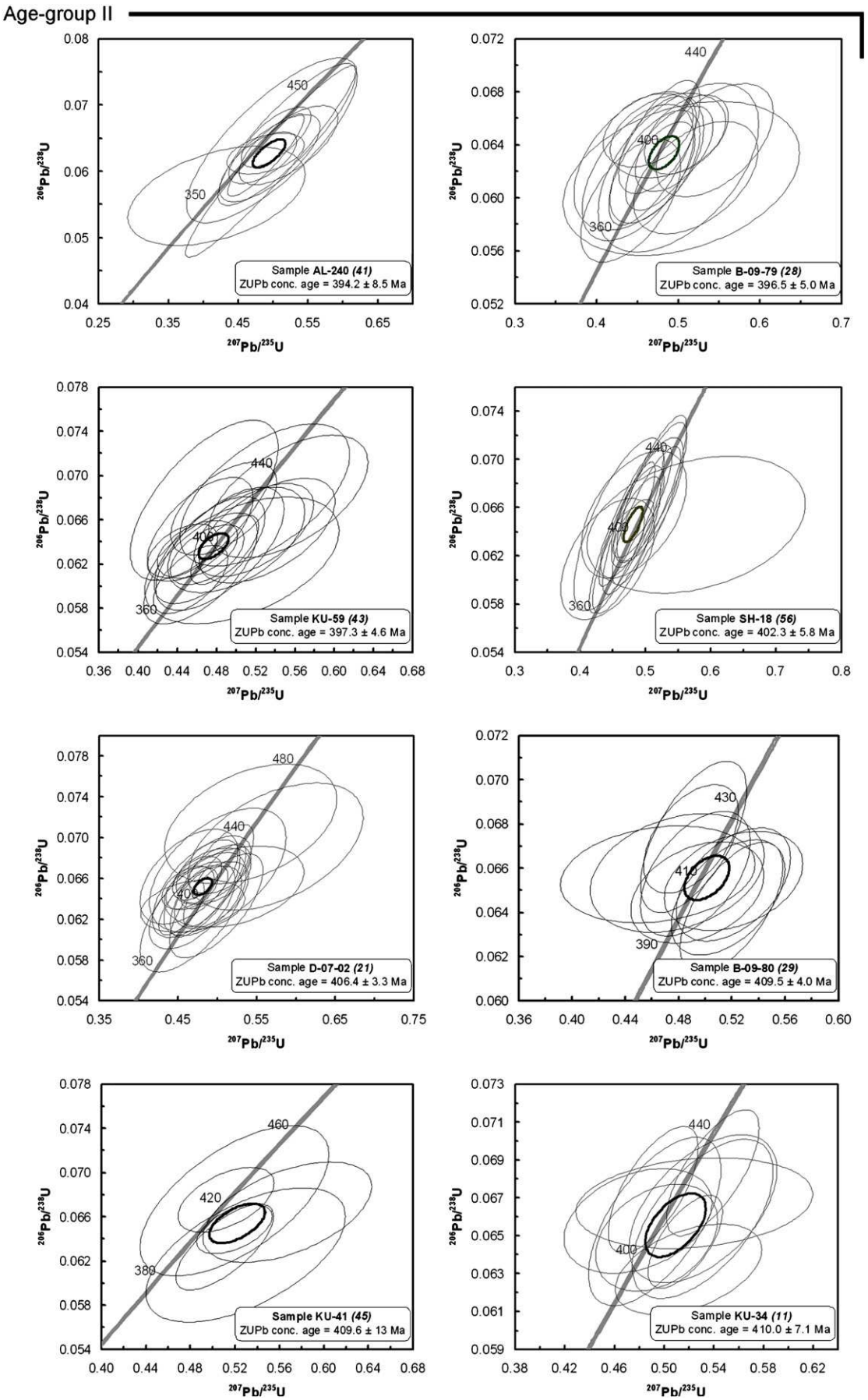


**Fig. 5.** (*continued*).

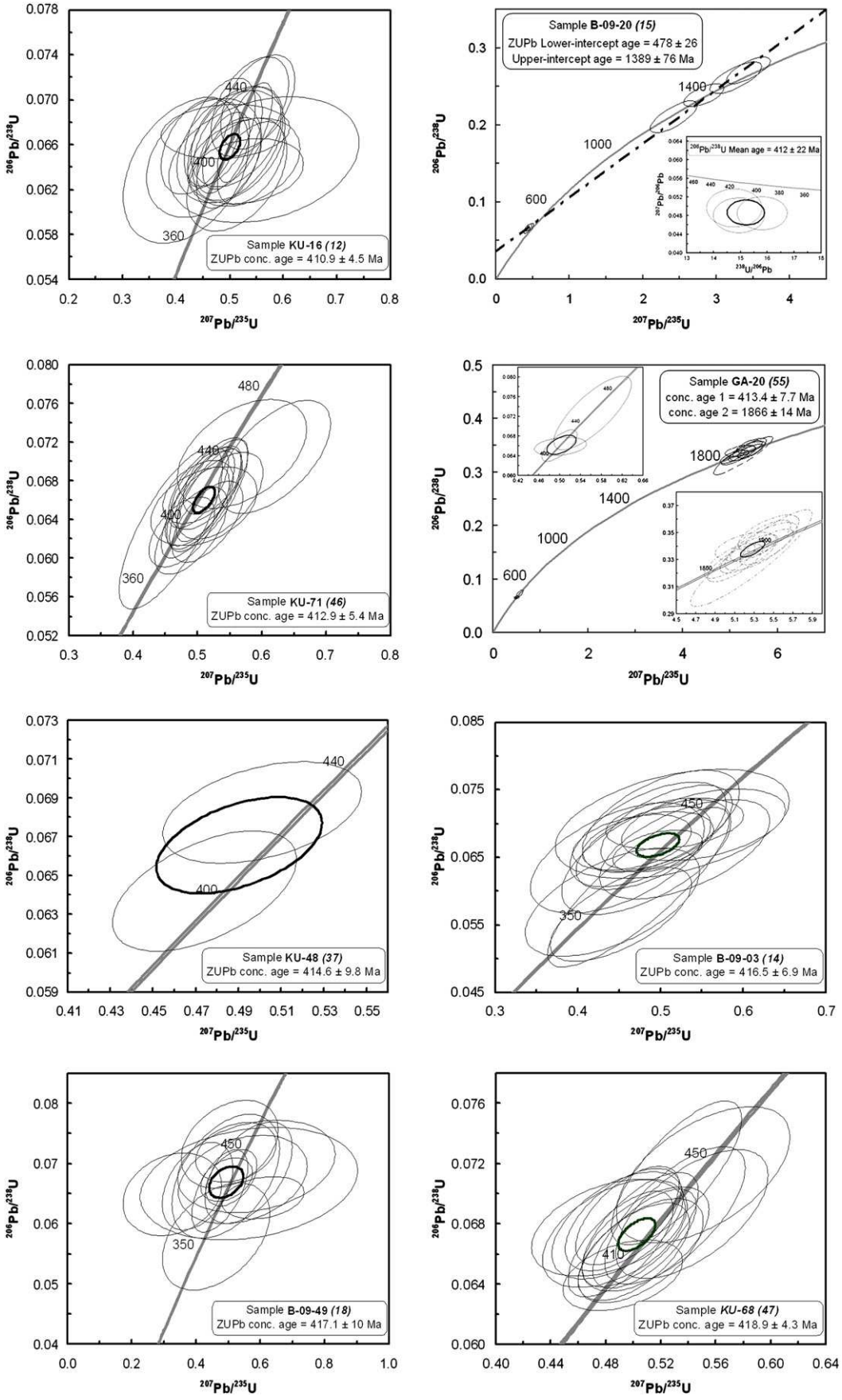


**Fig. 5.** (*continued*).

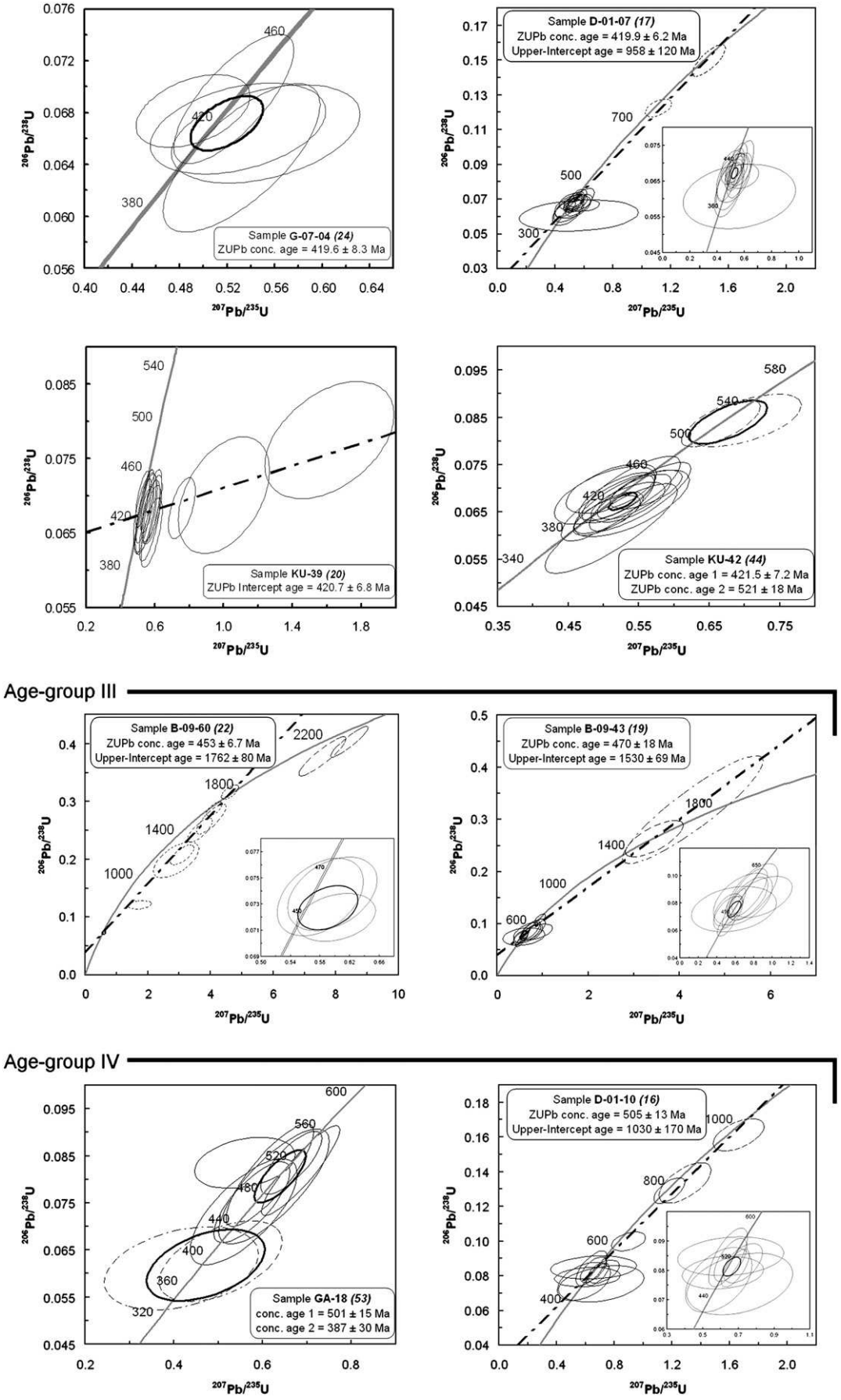


**Fig. 5.** (*continued*).

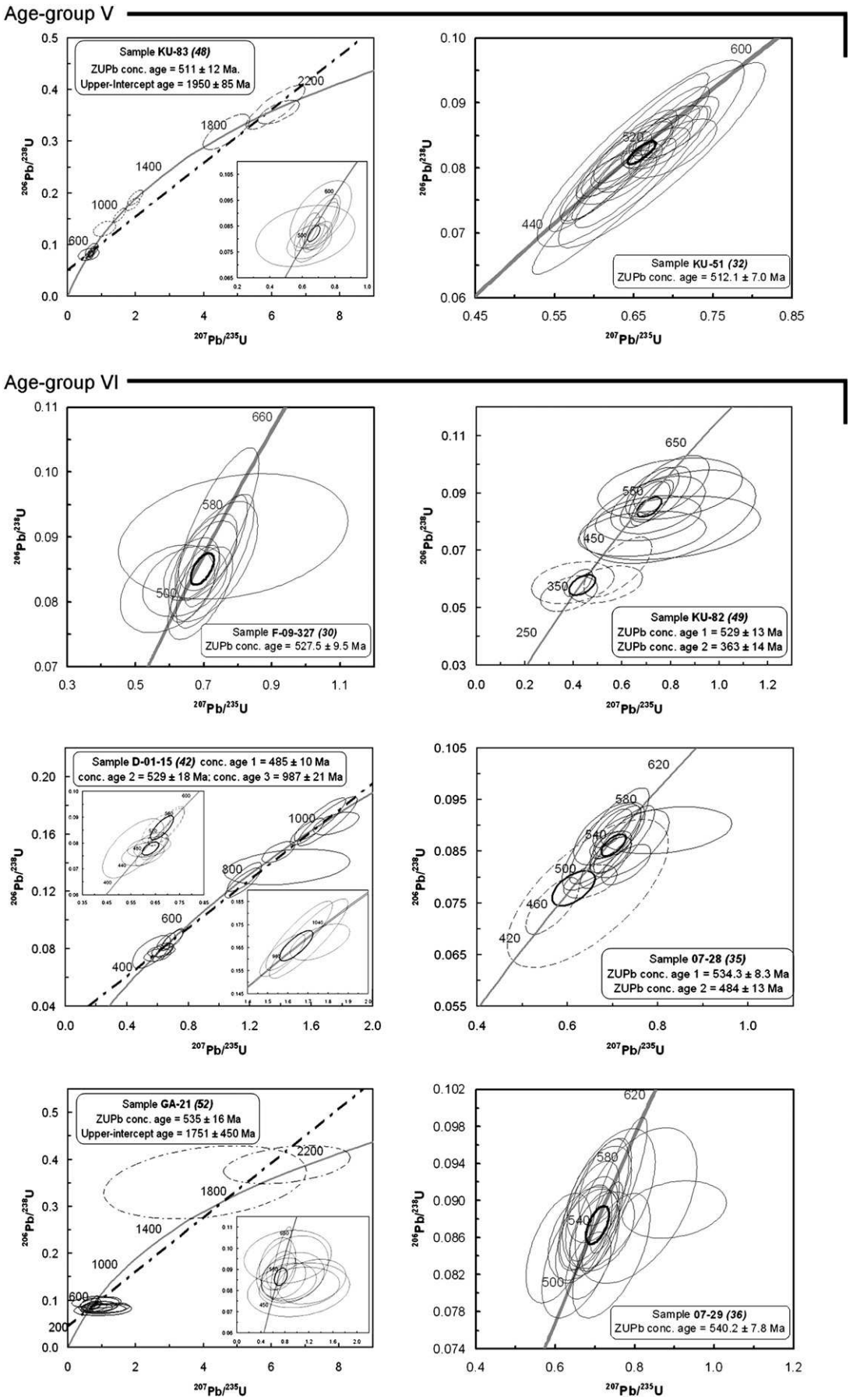


**Fig. 5.** (*continued*).

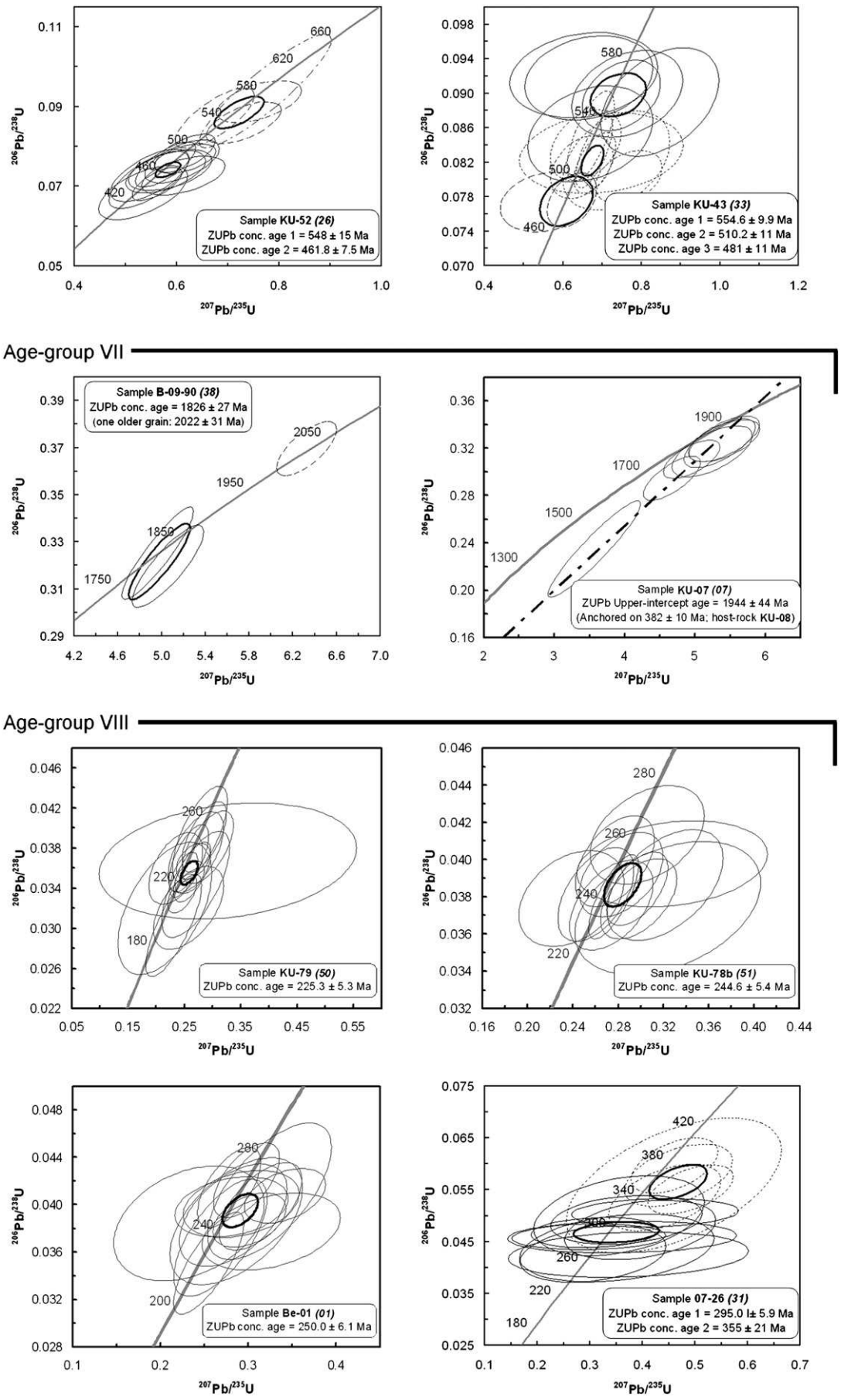


**Fig. 5.** (*continued*).

Table 1 summarises all analytical results. Average values over all analysed grains (excluding the outliers; <10%) are tabulated. A detailed table, listing the results for every grain analysed (except for the outliers) can be found in the data repository to this paper (Appendix 3). concordia plots are presented in Fig. 5 and their resulting U/Pb concordant or intercept ages are shown in Fig. 4. The concordia plots are listed chronologically following their age from young to old, except for the Late Palaeozoic (Permian) and Early Mesozoic (Triassic) samples that were emplaced after the GA–AM collision. The latter ages are listed at the end of the figure (Fig. 5). The numbers in italic and between brackets next to the age refer to the sample locations in Fig. 4.

The obtained ages range from the Late Palaeo–Proterozoic to the Early Mesozoic. They can be subdivided in eight distinctive age-groups (groups I–VIII, Fig. 5). Some samples yield two or three concordant components that correspond to different age-groups. Their distinction was made based on the resulting concordia-plot, aided by the difference in CL (Cathodoluminescence) characteristics of the analysed zircon populations. Fig. 6 shows some examples of CL-images for samples with two distinct zircon populations. The younger populations of samples KU-29 and KU-83 show obvious oscillatory magmatic zonation, which is clearly in contrast with the grains from the older population. For other samples, such as KU-82 and 07-26, the difference between both populations is more subtle.

Note that some zircon samples have very low U and Pb concentrations, resulting in low $^{206}Pb/^{204}Pb$ ratios (Table 1). This means that common-Pb becomes more important than can be corrected for, especially for $^{206}Pb/^{204}Pb$ ratios below 300 (samples KU-86 *(08)*; 07-26 *(31)*; GA-21 *(52)*). Corresponding with their low Pb-concentration, the $^{207}Pb$ signal is also low, resulting in a larger uncertainty on the $^{207}Pb/^{235}U$ age. In this case, the common-Pb presence is obscured due to the larger uncertainty-ellipse and the Isoplot programme can more easily calculate a concordant age while in reality, the data-points might be shifted from concordia. In other words, care should be taken when interpreting these ages for aforementioned samples as they might be slightly younger than they appear on the concordia plot.

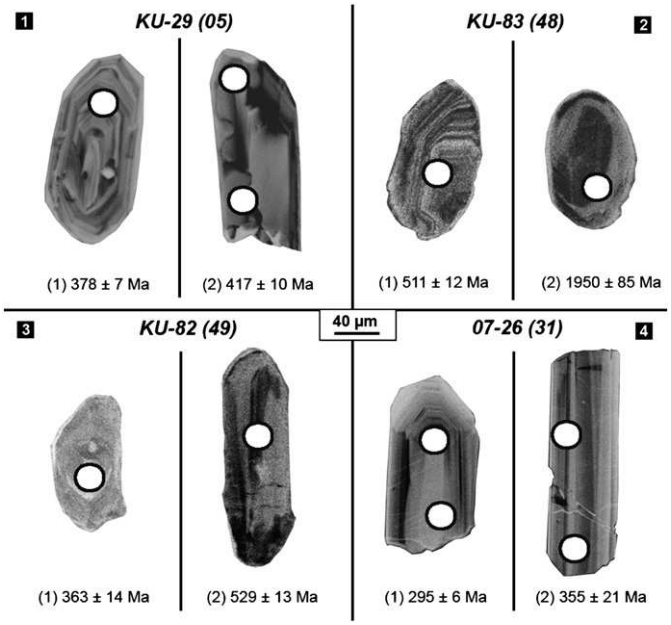


**Fig. 6.** Different types of zircon crystals occurring within one sample, as revealed by CL (Cathodoluminescence)-images. The younger populations of samples KU-29 and KU-83 show oscillatory magmatic zonation, which is clearly in contrast with the older population. For other samples such as KU-82 and 07-26, the difference between both populations is more subtle. Ablation targets are indicated in white.

In this paper, we follow the 2010 geological timescale by the International Commission on Stratigraphy which is based on the Gradstein et al. (2004) timescale.

### 4.1. Age-groups I, II and III: Devonian–Ordovician

Age-group I is represented by 16 samples with concordant ages ranging from ~395 to 360 Ma (Middle Devonian; Late Eifelian–Late Devonian; Famennian). Within this group, two samples KU-29 *(05)* and G-07-7 *(25)* yield a second concordant component of Late Silurian age (~425–416 Ma; Late Wenlock–Pridoli). Although this component is only represented by a few grains in each sample, it is consistent, and it indicates that assimilation of Late Silurian zircons was involved in the Devonian magma emplacement. These Late Silurian inherited ages correspond to primary emplacement ages of age-group II. This group covers 20 basement samples with concordant or lower-intercept ages of Late Silurian–Early Devonian age (~425–400 Ma; Homerian–Emsian). The first three samples shown in Fig. 5 yield concordant ages that are somewhat younger (~397–394 Ma; Eifelian) and overlap with older ages in group I. They can be regarded as a transitional group. Samples B-09-20 *(15)*, GA-20 *(55)* and D-01-07 *(17)* exhibit a Proterozoic age-component, reflecting reworking of older zircons. Note that these older zircons are only found north of the CTUSs (Fig. 4). The lower-intercept age of Sample B-09-20 *(15)* ($478 \pm 26$ Ma) is defined by three zircon grains only, which show reverse concordia. Based on this age, the sample should be assigned to age-group III (see Section 4.2). However, the position of the three points close to concordia on the provided Terra-Wasserburg plot might indicate that the grains are in fact younger. Therefore, we prefer to use the mean $^{206}Pb/^{238}U$ age ($412 \pm 22$ Ma) for these grains, corresponding to a group II crystallisation age. Given the sample location at the boundary zone of age-group II and III (Figs. 4; 7), no geological evidence can be used to exclude one of these possibilities. In sample KU-42 *(44)*, two older (Early Cambrian) grains were found.

Group III comprises two samples with a concordant Middle–Late Ordovician age (~470–450 Ma; Dapingian–Katian). Both samples also yield a Proterozoic upper-intercept age (Palaeo– to Meso–Proterozoic), similar to some samples in group II as discussed above. In principle, sample KU-52 *(26)* could also be included here, but because of its older component, it will be discussed later.

### 4.2. Age-groups IV, V, VI: Cambrian–Ediacaran

The Late Ediacaran–Cambrian samples are subdivided in groups IV, V and VI. Group IV is composed of two gneiss-samples with a main concordant Middle Cambrian age-component (~505–500 Ma). Sample GA-18 *(53)* contains two younger grains and sample D-01-10 *(16)* has some older grains that might define a discordia-line up to the Meso–Proterozoic. Samples KU-83 *(48)* and KU-51 *(32)* originate from felsic to intermediate pyroclastics or shallow intrusions that define age-group V (~510 Ma). Sample KU-83 exhibits Proterozoic components. Age-group VI is characterised by eight Ediacaran–Early Cambrian (~555–525 Ma) gabbroid and granitoid (tonalite–granodiorite) samples (D-01-15 *(42)* is an orthogneiss from a granitoid protolith). Some samples contain younger components which can be linked with age-group I: KU-82 *(49)*, age-group III: KU-52 *(26)*, age-group V: KU-43 *(33)* and/or an Early Ordovician age-group (~488–480 Ma; Tremadocian). This suggests (1) (partial) resetting of the zircons during later events (especially during the Tremadocian) and/or (2) incorporation of older grains in newly formed magma. Samples D-01-15 and GA-21 yield a Proterozoic age-component, similar to that found in some samples from the younger age-groups.

### 4.3. Outlier age-group VII: Palaeo–Proterozoic

In contrast with all other GA samples, B-09-90 *(38)* and KU-07 *(07)* entail a Palaeo–Proterozoic age-component. Therefore, they are

classified as "outlier-group VII". Only three zircons were found in the eclogite sample B-09-90 *(38)* and these exhibit an inherited Palaeo–Proterozoic signal. Sample KU-07 *(07)* originates from a mafic dike in the Chiket-aman granitic massif, which is dated by granite-granodiorite samples KU-08 (382 ± 4 Ma) and KU-86 (375 ± 10 Ma) (Table 1; Figs. 4, 5). Its zircon U/Pb data defines a discordia-line with a Palaeo–Proterozoic upper-intercept age and a meaningless lower-intercept age (597 ± 410 Ma). Therefore, we used the age of the granitic host-rock as an anchor to define the upper-intercept age with a better precision. The thus obtained age of 1944 ± 44 Ma can be interpreted as a maximum age of this Palaeo–Proterozoic age-component, since the dike intrusion age should clearly be younger than the granite host-rock crystallisation age.

### 4.4. Age-group VIII: Early Mesozoic–Late Palaeozoic

Age-group VIII defines the youngest samples of this study. Be-01 *(01)* and KU-79 *(50)* (KU-78b *(51)* as mafic enclave) are intra-plate granites with Late Permian–Triassic (225–220 Ma; Wuchapingian–Carnian) concordant ages. Sample 07-26 *(31)* was taken from a dioritic body which intruded along a sheared segment (Kurai-ridge, see further) of the CTUSs. The concordia plot for this sample yields two concordant age-components with the oldest component (Late Devonian) as an inherited signal reflecting age-group I. The youngest grains exhibit an Early Permian crystallisation age (295 ± 6 Ma). We suggest grouping this Early Permian sample together with the Early Mesozoic samples and not as a separate intrusion phase. Given its low $^{206}Pb/^{204}Pb$ ratio, the age might be overestimated (as discussed earlier) and therefore it might even tend closer to the Late Permian–Early Triassic ages.

## 5. Interpretation and discussion

In order to evaluate the regional distribution of the zircon U/Pb ages and to interpret them in a geodynamic context, a schematic map showing isochronological domains based on the above described age-groups is provided (Fig. 7).

### 5.1. Age-group I: Middle–Late Devonian GA–AM collision

The intrusions from age-group I (~395–360 Ma; Middle–Late Devonian) are found solely in the GA region or occur as narrow lenses within the CTUSs itself. These plutons were emplaced during the GA–AM collision and the ensuing formation of the complex mosaic-like structure of the CTUSs (Buslov et al., 2001, 2004; Dobretsov and Buslov, 2007). In general, somewhat older (Eifelian) intrusives (transitional age-group I and II) are found in the east along the Kurai-ridge segment of the CTUSs (Figs. 4, 8). This observation suggests that the Ob'-Zaysan oceanic branch of the PAO in between GA and AM (as part of Palaeo-Kazakhstan) closed diachronously from East to West (present-day co-ordinates). Hence, the Kazakhstan and Siberian continents migrated along a reactivated shear zone superimposed on the original ophiolitic CTUSs. These strike-slip movements reached peak-activity in the Late Devonian–Early Carboniferous and caused a fragmentation of the marginal part of the Siberian continent into several units (Uimon, Teletsk, Ulagan-Saratan, Erekta; Fig. 4) (Buslov et al., 2004). In the northern part of GA, Late Devonian–Early Carboniferous (360–350 Ma) ages were obtained (Vladimirov et al., 2001 and references therein) which are in agreement with the diachronous closure model of the Ob'-Zaisan part of the PAO, as is suggested here.

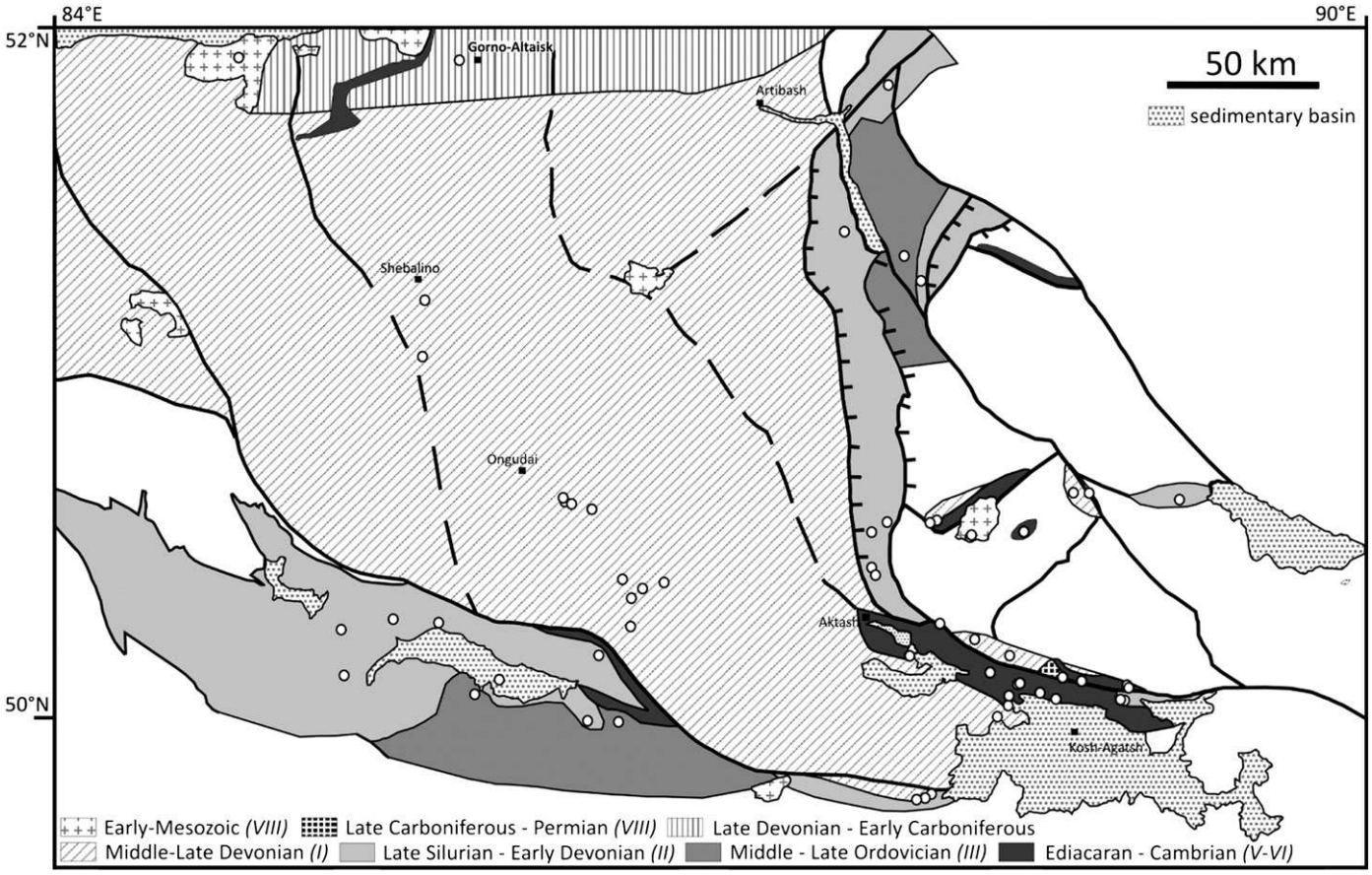


**Fig. 7.** Schematic map showing isochronological domains that refer to the discussed age-groups (see text). Outlier groups IV and VII are not shown.

### 5.2. Age-groups II and III: Ordovician–Early Devonian Palaeo-Kazakhstan assembly

The intrusions in the Uimon and Teletsk unit belong to a single Late Silurian–Early Devonian age-group (~425–400 Ma; group II) (Fig. 7). In the Teletsk unit, few published U/Pb data support our findings (Vladimirov et al., 2001 and references therein; De Grave et al., 2009). The intrusions located in the southeast of the Uimon-zone yielded Middle–Late Ordovician ages (~470–450 Ma; age-group III). One sample in the east of the Teletsk-unit gives a similar age of 460 ± 7 Ma (Fig. 4) (De Grave et al., 2009). This age suggests that the Uimon and Teletsk zones correspond to a single unit at the AM-margin, which was disrupted during the Late Palaeozoic collisions of AM and Palaeo-Kazakhstan with GA (Buslov et al., 2004). The Middle–Late Ordovician ages obtained there correspond to ages of many intrusions in West-Sayan and Tuva, located east of our study-area (Fig. 1) (e.g. 483–413 Ma; Distanova, 2000 and references therein) and in the Chinese Altai (southern margin of AM; 451–433 Ma; Briggs et al., 2007). They were emplaced during the assembly of Palaeo-Kazakhstan and are formed in the Kazakhstan–Tuva–Mongolia island-arc environment (Dobretsov and Buslov, 2007; Kröner et al., 2007). In more detail, the Late Silurian–Early Devonian age-group (II) can be linked with the accretion of an island-arc to the southern margin of AM in the Chinese Altai (present-day co-ordinates) (Windley et al., 2002; Wang et al., 2006). According to Wang et al. (2006), an extensive volume of granitoids was emplaced and deformed during this period (~415–400 Ma) in both the island-arc system and the AM microcontinent. The origin of this island-arc is debatable. In the model of Yuan et al. (2007), the Late Silurian–Early Devonian magmatism is attributed to the emplacement of mantle-derived magma in an extensional continental margin setting as has occurred in the modern analogue of Baja California for example. The two older gneiss-samples (~505 Ma; age-group IV) correspond to data from Kuznetsk-Alatau (Rudnev et al., 2008) and West-Sayan (Rudnev et al., 2004) and might reflect older events in the Palaeo-Kazakhstan amalgamation.

### 5.3. Proterozoic ages: Reworked ancient crust in Palaeo-Kazakhstan

Both age-groups II and III show Proterozoic age-components which support the model that the formation of juvenile mantle-derived magma in AM involves limited assimilation of older crustal material (Yuan et al., 2007). Upper-intercept ages for these samples are in agreement with the model Sm/Nd ages of Kruk et al. (2010): 1.0–0.8 Ga in the CTUSs (island-arc protoliths) and 1.6–1.4 in the AM-periphery (AM-margin protoliths, Figs. 4, 5). Some samples exhibit older components between 2.0 and 1.8 Ga. Within the CAOB framework, similar Late Palaeo–Proterozoic ages were found e.g. in the Tuva–Mongolian and Southern Gobi microcontinents (Kozakov et al., 1999; Demoux et al., 2009). These ages can be linked with protoliths, formed during the Late Palaeo–Proterozoic world-wide crust formation, related with the amalgamation of the supposed Pre-Rodinian (Columbia) supercontinent (e.g. Kröner, 1991; Zhao et al., 2002, 2006; Hou et al., 2008).

The Palaeo–Proterozoic age-components of outlier-group VII do not reflect any direct Gondwana-affinity within GA before the GA–AM collision. B-09-90 *(38)* was sampled in the Chagan-Uzun high-pressure metamorphic complex, which formed in an intra-oceanic arc-trench system (Fig. 8). The protoliths are thought to be oceanic plateaus and seamounts that subducted under a primitive island-arc (discussed in Section 5.4; Ota et al., 2007). Previous studies showed that these protoliths contain a recycled crustal component (Safonova et al., 2009; Utsunomiya et al., 2009) as indicated by our inherited zircon U/Pb data. Sample KU-07 is a mafic dike in the Late-Devonian Chiket-aman massif, which was hence emplaced after the collision of GA and AM.

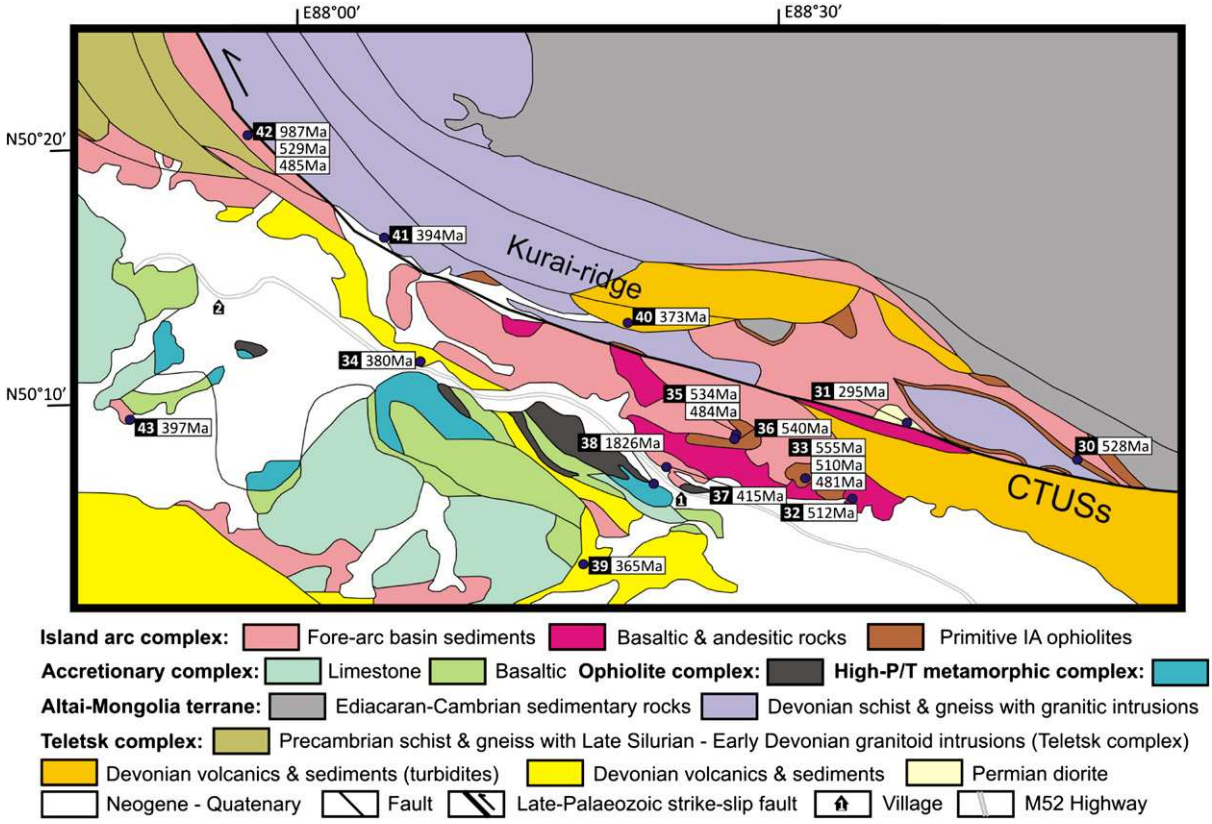


**Fig. 8.** Geological map of the Kurai–Chagan-Uzun–Chuya region where sampling occurred more extensively (after Buslov et al., 1993; Ota et al., 2007). Zircon U/Pb ages are indicated. We interpret the geological units of this area in the context of the formation and evolution of the Kuznetsk-Altai island-arc (see text and Fig. 2). Village 1 = Chagan-Uzun, 2 = Kurai.

### 5.4. Age groups IV, V, VI: Ediacaran–Cambrian Gorny Altai assembly

Ediacaran–Early Ordovician ages (age-groups IV–V–VI) are found in ophiolite rocks along the CTUSs. They are interpreted in the context of the formation and evolution of the Kuznetsk-Altai island-arc at the margin of the Siberian continent (Buslov et al., 2002; Ota et al., 2007). The key-area to understand the evolution of this island-arc system is the Kurai–Chagan-Uzun–Chuya region, where we hence sampled most densely (Fig. 4). The geology of this area is presented in Figs. 2 and 8 (after Buslov et al., 1993; Ota et al., 2007). As shown, three important terranes can be identified. The accretionary complex consists of a basalt-dominated unit with OIB and MORB signatures (Safonova et al., 2004, 2008). These seamount/oceanic plateau basalts are capped by a limestone-dominated unit (palaeo-atoll) with a Pb/Pb isochron age of 598 ± 25 Ma (Uchio et al., 2008). They represent seamounts that were dragged into the PAO-Siberia subduction zone, simultaneously with the formation of an incipient island-arc system, close to the Siberian margin. Seamount relics are found in the OP (ophiolitic) and HP (High-Pressure/Temperature metamorphic) complex of the Kurai–Chagan-Uzun–Chuya area. The OP-complex consists of serpentinized peridotite and gabbro–amphibolite, intruded by gabbroid and pyroxenite dikes and overprinted by island-arc volcanism. The HP-complex exhibits eclogite facies metamorphism, which is dated by amphibole $^{40}Ar/^{39}Ar$ at 636–627 Ma (Fig. 8) (Buslov et al., 2002; Ota et al., 2007). Eclogite sample B-09-90 *(38)* originates from this HP-terrane, and as discussed earlier, its few zircons yielded only Palaeo–Proterozoic ages. This observation confirms that the oceanic plateaus in GA contain a recycled crustal component (Safonova et al., 2009; Utsunomiya et al., 2009).

In the north (present-day co-ordinates) of these units, juvenile continental crust of the Kuznetsk-Altai island-arc was formed during two stages. First a primitive island-arc was formed, which is characterised by boninite–tholeiite volcanic series, similar to the Izu-Bonin islands. This early stage of arc-development was later overprinted by tholeiitic and calc-alkaline volcanics of a more evolved island-arc (Buslov et al., 2001, 2002). The gabbroid and granitoid samples of age-group VI (Ediacaran–Early Cambrian; ~555–525 Ma) are located within the island-arc complex and are therefore associated with primitive-arc formation, as outlined above. The Middle Cambrian tuffs (~510 Ma; age-group V) can be linked to volcanism of the evolved calc-alkaline magmatic arc. Similar conclusions were drawn for the Kuznetsk-Alatau segment of the Kuznetsk-Altai island-arc. In this latter region, the first stage of arc-development is expressed by tholeiitic magmatism at ~530 Ma, followed by calc-alkaline and subalkaline magmatism at ~500 Ma (Rudnev et al., 2008). The Early-Ordovician (~488–480 Ma, Tremadocian) age-component, exhibited by several samples, is contemporaneous with the formation of blueschists in contact with ophiolites of the Uimon zone (~492–485 Ma; phengite and glaucophane Ar/Ar; Volkova et al., 2005; Volkova and Sklyarov, 2007). These blueschists are also found in association with primitive island-arc ophiolites from the Kurai-ridge (Fig. 8) and Ulagan (Fig. 4). They were probably exhumed after the accretion of seamounts to the island-arc, which blocked the subduction zone. This observation might indicate that the Kuznetsk-Altai island-arc was consumed at that time. The gneiss-samples of age-group IV probably record regional metamorphism associated with this event.

Sample KU-82 (49) yields, besides its Early Cambrian primitive island-arc age, a secondary Late Devonian (363 ± 14 Ma) age-component (Fig. 5). The zircons that exhibit this younger age define a population of oscillatory zoned magmatic zircons with a lower CL-intensity than the older zircons (Fig. 6). The occurrence of a Late Devonian (367 ± 10 Ma) gabbroid sample (GA-07) at the boundary of the same unit might indicate that the secondary younger component defines the crystallisation age of gabbro KU-82 *(49)*. In this case, the majority of the zircon grains in the gabbro are exotic zircons, that presumably formed in an island-arc environment. The gabbro emplacement can then be linked with Late Devonian strike-slip movements, posterior to the GA–AM collision (Pirajno, 2010). More data are necessary in order to evaluate this hypothesis.

### 5.5. Age group VIII: Post-collisional intrusions

After the final Late Carboniferous–Permian collision of Palaeo-Kazakhstan with Siberia and Baltica, the CTUSs was reactivated as a large-scale strike-slip fault zone (Buslov et al., 2001, 2004). According to Pirajno (2010), suture-shear zones, which are weakened by strike-slip movements are able to channel mantle material into the sub-continental lithosphere. The occurrence of a Late Carboniferous–Permian (295 ± 6 Ma) diorite along the Kurai-ridge segment of the CTUSs (Fig. 8) might be explained in this geodynamic context, but as discussed earlier, this age might be slightly overestimated. The Late Permian–Triassic (255–220 Ma) granitoids of age-group VIII occur as small bodies in the entire ASFB (Fig. 4). They formed in an intra-plate context with an uncertain origin. Several authors attribute these intra-plate granitoids to the Siberian mantle-plume activity (Dobretsov, 2005; Pirajno, 2010). Alternatively, a model of slab break-off can be proposed for the origin of the Late Permian–Triassic granitoids. This model has been described earlier for many post-collisional plutons in orogenic belts around the world, suggesting that the granitoids are derived from mantle wedges that had previously been metasomatised by earlier subduction zones and magmatic arcs (e.g. Wu et al., 2002; Pin et al., 2008; Yuan et al., 2010).

## 6. Comparison with the adjacent Chinese and Mongolian Altai

At the southern edges of the ASFB, Altai-Mongolia is bordered by the Junggar block and the Chinese and Mongolian Altai Orogenic belts. In both belts, extensive Palaeozoic granitoid magmatism took place as the result of multiple subduction–accretion events (Badarch et al., 2002; Windley et al., 2002; Wang et al., 2006; Briggs et al., 2007; Yuan et al., 2007; Xiao et al., 2009; Long et al., 2010). The Chinese Altai is commonly subdivided into six NW–SE striking tectonic units, parallel to the bordering Erqis fault (also known as Ertix fault; Briggs et al. (2007) or Irtysh fault; Buslov et al. (2004)) in the South (Windley et al., 2002; Xiao et al., 2004). The northern Chinese Altai (unit 1) is mainly composed of Devonian volcanics, formed in an island-arc setting. The central Chinese Altai (units 2 and 3) is considered as the microcontinental part of Altai-Mongolia (with Precambrian basement) on which an Ordovician Andean-type arc was built. The southern Chinese Altai (units 4, 5, and 6) constitutes a Late Silurian–Early Devonian and a Devonian–Carboniferous island-arc complex (Windley et al., 2002; Xiao et al., 2004; Wang et al., 2009).

The major subduction–accretion processes in the Chinese Altai occurred between the Late Cambrian to the Middle Devonian (Windley et al., 2002; Xiao et al., 2004; Wang et al., 2006, 2009; Xiao et al., 2009). Resulting granitoid magmatism started in the Middle–Late Ordovician (~460 Ma) and reached a peak in the Late Silurian–Early Devonian (~410 Ma) (Wang et al., 2006, 2009; Long et al., 2010). Most granitoids in the northern and central Chinese Altai yielded zircon U/Pb ages of 416–399 Ma (Wang et al., 2006; Yuan et al., 2007; Wang et al., 2009 and references therein), which is in excellent agreement with the granitoids of age-group II (~425–400 Ma), presented in this study. The older (~465-450) granitoids in this area (Briggs et al., 2007; Wang et al., 2009) are mainly found in the southern Chinese Altai, which correspond well with the age-group III granitoids in Altai-Mongolia from our data. The tectonic setting of the Chinese Altai changed to post-orogenic in the Late Carboniferous–Early Permian (~290–270 Ma) and intraplate in the Mesozoic (~255–210 Ma) (Briggs et al., 2007; Wang et al., 2009). These ages are mimicked as well in our results and correspond well with those for the post-collisional and intraplate granitoids of age-group VIII.

Although a sufficient amount of age data was obtained for several regions in Mongolia (e.g. Demoux et al., 2009; Jian et al., 2010; Rojas-Agramonte et al., 2011), absolute age information for the Mongolian Altai, adjacent to our study area is limited. The Mongolian Altai borders the Tuva–Mongolia microcontinent to the east of our study area and is predominantly composed of a thick metamorphosed Cambrian–Ordovician succession of clastic and volcaniclastic rocks, which were deposited in an arc-proximal setting. The succession is intruded by calc-alkaline granitoid plutons, which were dated at 456-400 Ma by K–Ar dating (Badarch et al., 2002 and references therein). Kröner et al. (2007) report similar (~460-415 Ma) zircon U–Pb ages on felsic igneous rocks with island-arc affinity from several regions in northern and central Mongolia, close to the Tuva–Mongolian border.

## 7. Conclusions and summarising tectonic model

The zircon U/Pb data from the Charysh–Terekta–Ulagan–Sayan suture (CTUSs) presented here are interpreted in terms of the multi-stage tectonic evolution of the PAO (Fig. 9). In the Late Proterozoic–Early Palaeozoic, the current western part of Siberia was bordered by two major magmatic arcs, which were separated by the Ob'-Zaisan branch of the PAO. The Kuznetsk-Altai island-arc was located close to the Siberian margin, while the Kazakhstan–Tuva–Mongolian island-arc was closer to Gondwana, where it collided with Gondwana-derived microcontinents to form the Kazakhstan-Baikal composite continent or Palaeo-Kazakhstan. These island-arc systems are the main contributors to the formation of juvenile continental crust within the ASFB. The main stages of magmatic activity in this context can be summarised as follows:

1) In Gorny Altai (GA) gabbroid and granitoid (tonalite–granodiorite) samples reveal that primitive arc crust of the future Kuznetsk-Altai arc was formed close to the Siberian margin during the Ediacaran–Early Cambrian (555–525 Ma). As recorded by zircons in felsic tuffs, this Kuznetsk-Altai magmatic arc developed further during the Middle–Late Cambrian (~510 Ma). In the Late Cambrian–Early Ordovician (490–480 Ma), the island-arc was being consumed in

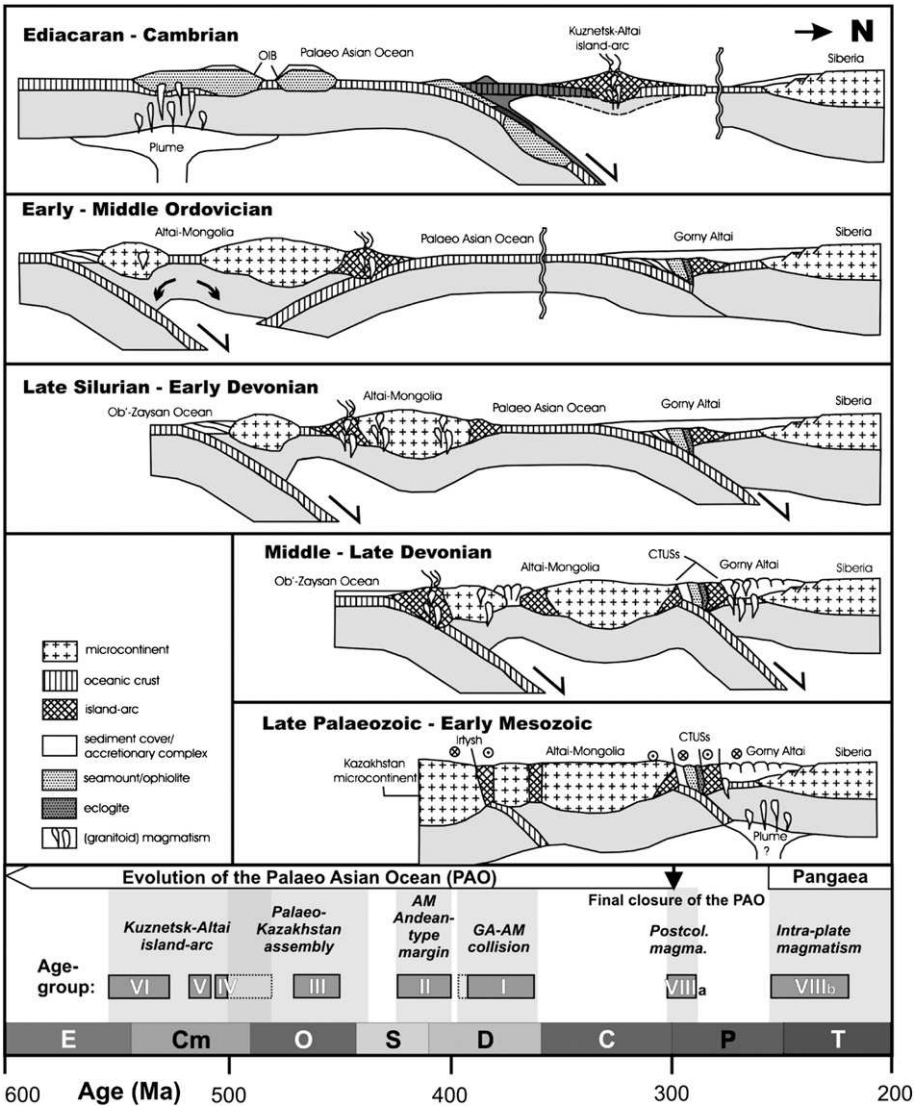


**Fig. 9.** (Top panels) Schematic tectonic model for the Palaeozoic evolution of the CTUSs (based on Buslov et al., 1993; Windley et al., 2002; Buslov et al., 2004; Wang et al., 2006; Briggs et al., 2007; Ota et al., 2007). (Bottom panel) Illustration and interpretation of the obtained age-groups in their specific geodynamic context. Dotted boundaries mark a possibly prolonged duration of events I (Eifelian samples) and IV (Tremadocian age-components). The oldest ages (IV–V–VI) were obtained for intrusions of the Kuznetsk-Altai island-arc, where age-group IV marks the start of the GA–Siberia collision. In the same period, Altai-Mongolia (Palaeo-Kazakhstan in a broader context) assembled in a more distal environment from Siberia. Magmatic event II can be interpreted as a result of an Andean-type collision with AM at the Palaeo-Kazakhstan margin. During the progressive PAO consumption, GA and AM collided, which resulted in the intrusion of numerous plutons in GA. After the final PAO closure, GA experienced post-collisional and intra-plate magmatism, resulting in the intrusives of age-group VIII. Pre-Ediacaran events (age-group VII) are not shown on the figure.

the subduction zone forming the Siberian Early Caledonian accretion–collision belt.

2) During the Ordovician, the Palaeo-Kazakhstan microcontinent was assembled. The Middle–Late Ordovician ages (470–450 Ma) obtained at the margin of Gondwana-derived Altai-Mongolia (AM) are associated with this episode of Palaeo-Kazakhstan assembly. In the Uimon and Teletsk units, located at the AM-margin, Silurian–Early Devonian ages (425–400 Ma) were obtained from the igneous basement which can be related to an Andean-type collision, possibly after a short extensional episode. Occasional Palaeo–Proterozoic ages suggest that reworked ancient crust contributed to the growth of Palaeo-Kazakhstan.
3) In the Middle–Late Devonian (395–360 Ma), voluminous granitoids were emplaced as a result of the collision of AM with GA. This collision also led to large-scale Late Devonian–Early Carboniferous strike-slip displacements along the CTUSs. Continuous closure of the PAO and the Late Carboniferous–Permian collision of Baltica, Siberia and Palaeo-Kazakhstan resulted in strike-slip reactivation of the CTUSs and the emplacement of mantle-derived magma (~295 Ma).

The youngest granitoids (255–220 Ma) sampled from this region were formed after Pangaea assembly and record Permian–Triassic intra-plate magmatism.

Supplementary materials related to this article can be found online at doi:10.1016/j.gr.2011.03.003.

## Acknowledgements

The authors were supported by grants of the Institute for the Promotion of Innovation through Science and Technology in Flanders (IWT-Vlaanderen) (SG) and the Fund for Scientific Research — Flanders (FWO, Belgium) (JDG). This research was also jointly funded by Ghent University (BOF — bilateral project 01SB1309) and by the integration programme of the ONZ RAN (grant N 10.2 and scientific school 65804.2010.5). We are indebted to W. Xiao, I.Y. Safonova and an anonymous reviewer for their insightful suggestions and constructive reviews.

## References

Avrov, D.P., 1978. Geological map of the USSR, scale 1:1,000,000, sheet M-(44), 45 (Ust-Kamenogorsk), In: Avrov, D.P. (Ed.). Ministry of Geology, USSR, Moscow.

Badarch, G., Cunningham, W.D., Windley, B.F., 2002. A new terrane subdivision for Mongolia: implications for the Phanerozoic crustal growth of Central Asia. Journal of Asian Earth Sciences 21, 87–110.

Belousova, E.A., Kostitsyn, Y.A., Griffin, W.L., Begg, G.C., O'Reilly, S.Y., Pearson, N.J., 2010. The growth of the continental crust: constraints from zircon Hf-isotope data. Lithos 119, 457–466.

Briggs, S.M., Yin, A., Manning, C.E., Chen, Z.L., Wang, X.F., Grove, M., 2007. Late Paleozoic tectonic history of the Ertix fault in the Chinese Altai and its implications for the development of the Central Asian Orogenic System. Geological Society of America Bulletin 119, 944–960.

Buslov, M.M., 2011. Tectonics and geodynamics of the Central Asian Foldbelt: the role of Late-Palaeozoic large-amplitude displacements. Russian Geology and Geophysics 52, 66–90.

Buslov, M.M., Watanabe, T., 1996. Intrasubduction collision and its role in the evolution of an accretionary wedge: the Kurai zone of Gorny Altai, Central Asia. Russian Geology and Geophysics 36, 83–94.

Buslov, M.M., Berzin, N.A., Dobretsov, N.L., Simonov, V.A., 1993. Geology and tectonics of Gorny Altai. In: Dobretsov, N.L. (Ed.), Guide-book for the Post-symposium Excursion of the 4th International Symposium of the IGCP project 283: "Geodynamic Evolution of the Paleoasian Ocean". SB-RAS Novosibirsk.

Buslov, M.M., Safonova, I.Y., Watanabe, N., Obut, O.T., Fujiwara, I., Iwata, K., Semakov, N.N., Sugai, Y., Smirnova, L.V., Kazanskii, A.Y., 2001. Evolution of the Palaeo-Asian Ocean (Altai-Sayan Region, Central Asia) and collision of possible Gondwana-derived terranes with the southern marginal part of the Siberian continent. Geosciences Journal 5, 203–204.

Buslov, M.M., Watanabe, T., Saphonova, I.Y., Iwata, K., Travin, A., Akiyama, M., 2002. A Vendian–Cambrian island arc system of the Siberian continent in Gorny Altai (Russia, Central Asia). Gondwana Research 5, 781–800.

Buslov, M.M., Watanabe, T., Fujiwara, Y., Iwata, K., Smirnova, L.V., Safonova, I.Y., Semakov, N.N., Kiryanova, A.P., 2004. Late Paleozoic faults of the Altai region, Central Asia: tectonic pattern and model of formation. Journal of Asian Earth Sciences 23, 655–671.

De Grave, J., Buslov, M.M., Van den Haute, P., Metcalf, J., Dehandschutter, B., McWilliams, M.O., 2009. Multi-method chronometry of the Teletskoye graben and its basement, Siberian Altai Mountains: new insights on its thermo-tectonic evolution. In: Lisker, F., Ventura, B., Glasmacher, U.A. (Eds.), Thermochronological Methods — From Palaeotemperature Constraints to Landscape Evolution Models: Geological Society Special Publication, London, pp. 237–259.

Demoux, A., Kroner, A., Liu, D.Y., Badarch, G., 2009. Precambrian crystalline basement in southern Mongolia as revealed by SHRIMP zircon dating. International Journal of Earth Sciences 98, 1365–1380.

Distanova, A.N., 2000. Early Paleozoic granitoid associations of the Altai-Sayan folded area: their types and importance in paleogeodynamic reconstructions. Russian Geology and Geophysics 41, 1244–1257.

Dobretsov, N.L., 2005. 250 Ma large igneous provinces of Asia: Siberian and Emeishan traps (plateau basalts) and associated granitoids. Russian Geology and Geophysics 46, 847–868.

Dobretsov, N.L., Buslov, M.M., 2007. Late Cambrian–Ordovician tectonics and geodynamics of Central Asia. Russian Geology and Geophysics 48, 71–82.

Dobretsov, N.L., Buslov, M.M., Vernikovsky, V.A., 2003. Neoproterozoic to Early Ordovician evolution of the Paleo-Asian Ocean: implications to the break-up of Rodinia. Gondwana Research 6, 143–159.

Dobretsov, N.L., Buslov, M.M., Yu, U.C., 2004. Fragments of oceanic islands in accretion–collision areas of Gorny Altai and Salair, southern Siberia, Russia: early stages of continental crustal growth of the Siberian continent in Vendian–Early Cambrian time. Journal of Asian Earth Sciences 23, 673–690.

Dunkl, I., Mikes, T., Frei, D., Gerdes, A., von Eynatten, H., 2009. PepiAGE: Data Reduction Program for Time-resolved U/Pb Analyses — Introduction and Call for Tests and Discussion. University of Goettingen Publication. 15 pp. http://www.sediment.uni-goettingen.de/staff/dunkl/zips/PepiAGE-introduction-c1.pdf.

Frei, D., Gerdes, A., 2009. Precise and accurate in situ U–Pb dating of zircon with high sample throughput by automated LA-SF-ICP-MS. Chemical Geology 261, 261–270.

Gerdes, A., Zeh, A., 2009. Zircon formation versus zircon alteration — new insights from combined U–Pb and Lu–Hf in-situ LA-ICP-MS analyses, and consequences for the interpretation of Archean zircon from the Central Zone of the Limpopo Belt. Chemical Geology 261, 230–243.

Glorie, S., De Grave, J., Buslov, M.M., Elburg, M.A., Stockli, D.F., Gerdes, A., Van den haute, P., 2010. Multi-method chronometric constraints on the evolution of the Northern Kyrgyz Tien Shan granitoids (Central Asian Orogenic Belt): from emplacement to exhumation. Journal of Asian Earth Sciences 38, 131–146.

Gradstein, F.M., Ogg, J.G., Smith, A.G., Bleeker, W., Lourens, L.J., 2004. A new Geologic Time Scale, with special reference to Precambrian and Neogene. Episodes 27, 83–100.

Hou, G.T., Santosh, M., Qian, X.L., Lister, G.S., Li, J.H., 2008. Configuration of the Late Paleoproterozoic supercontinent Columbia: insights from radiating mafic dyke swarms. Gondwana Research 14, 395–409.

Isozaki, Y., Aoki, K., Nakama, T., Yanai, S., 2010. New insight into a subduction-related orogen: a reappraisal of the geotectonic framework and evolution of the Japanese Islands. Gondwana Research 18, 82–105.

Jackson, S.E., Pearson, N.J., Griffin, W.L., Belousova, E.A., 2004. The application of laser ablation-inductively coupled plasma-mass spectrometry to in situ U–Pb zircon geochronology. Chemical Geology 211, 47–69.

Jahn, B.M., 2004. The Central Asian Orogenic Belt evolution and growth of the continental crust in the Phanerozoic. In: Malpas, J., Fletcher, C.J.N., Ali, J.R., Aichison, J.C. (Eds.), Aspects of the Tectonic Evolution of China: Geological Society of London, Special Publication, 226, pp. 73–100. London.

Jahn, B.M., Wu, F.Y., Hong, D.W., 2000. Important crustal growth in the Phanerozoic: isotopic evidence of granitoids from east-central Asia. Proceedings of the Indian Academy of Sciences—Earth and Planetary Sciences 109, 5–20.

Jian, P., Kroner, A., Windley, B.F., Shi, Y.R., Zhang, F.Q., Miao, L.C., Tomurhuu, D., Zhang, W., Liu, D.Y., 2010. Zircon ages of the Bayankhongor ophiolite melange and associated rocks: time constraints on Neoproterozoic to Cambrian accretionary and collisional orogenesis in Central Mongolia. Precambrian Research 177, 162–180.

Khain, E.V., Bibikova, E.V., Salnikova, E.B., Kröner, A., Gibsher, A.S., Didenko, A.N., Degtyarev, K.E., Fedotova, A.A., 2003. The Palaeo-Asian ocean in the Neoproterozoic and early Palaeozoic: new geochronologic data and palaeotectonic reconstructions. Precambrian Research 122, 329–358.

Kovalenko, V.I., Yarmolyuk, V.V., Kovach, V.P., Kotov, A.B., Kozakov, I.K., Salnikova, E.B., Larin, A.M., 2004. Isotope provinces, mechanisms of generation and sources of the continental crust in the Central Asian mobile belt: geological and isotopic evidence. Journal of Asian Earth Sciences 23, 605–627.

Kozakov, I.K., Kotov, A.B., Sal'nikova, E.B., Bibikova, E.V., Kovach, V.P., Kirnozova, T.I., Berezhnaya, N.G., Lykhin, D.A., 1999. Metamorphic age of crystalline complexes of the Tuva–Mongolia Massif: the U–Pb geochronology of granitoids. Petrology 7, 177–191.

Kröner, A., 1991. Tectonic evolution in the Archean and Proterozoic. Tectonophysics 187, 393–410.

Kröner, A., Windley, B.F., Badarch, G., Tomurtogoo, O., Hegner, E., Jahn, B.M., Gruschka, S., Khain, E.V., Demoux, A., Wingate, M.T.D., 2007. Accretionary growth and crust formation in the Central Asian Orogenic Belt and comparison with the Arabian–Nubian shield. Geological Society of America Memoirs Memoir 200, 181–209.

Kruk, N.N., Vladimirov, A.G., Babin, G.A., Shokalsky, S.P., Sennikov, N.V., Rudnev, S.N., Volkova, N.I., Kovach, V.P., Serov, P.A., 2010. Continental crust in Gorny Altai: nature and composition of protoliths. Russian Geology and Geophysics 51, 431–446.

Long, X.P., Yuan, C., Sun, M., Xiao, W.J., Zhao, G.C., Wang, Y.J., Cai, K.D., Xia, X.P., Xie, L.W., 2010. Detrital zircon ages and Hf isotopes of the early Paleozoic flysch sequence in

the Chinese Altai, NW China: new constrains on depositional age, provenance and tectonic evolution. Tectonophysics 480, 213–231.
Ludwig, K., 2003. User's manual for Isoplot 3.00. A Geochronological Toolkit for Microsoft Excel: Berkeley Geochronology Center Special Publication, v. 4.
Ota, T., Utsunomiya, A., Uchio, Y., Isozaki, Y., Buslov, M.M., Ishikawa, A., Maruyama, S., Kitajima, K., Kaneko, Y., Yamamoto, H., Katayama, I., 2007. Geology of the Gorny Altai subduction–accretion complex, southern Siberia: tectonic evolution of an Ediacaran–Cambrian intra-oceanic arc-trench system. Journal of Asian Earth Sciences 30, 666–695.
Pin, C., Fonseca, P.E., Paquette, J.L., Castro, P., Matte, P., 2008. The ca. 350 Ma Beja Igneous Complex: a record of transcurrent slab break-off in the Southern Iberia Variscan Belt? Tectonophysics 461, 356–377.
Pirajno, F., 2010. Intracontinental strike-slip faults, associated magmatism, mineral systems and mantle dynamics: examples from NW China and Altay-Sayan (Siberia). Journal of Geodynamics 50, 325–346.
Rojas-Agramonte, Y., Kröner, A., Demoux, A., Xia, X., Wang, W., Donskaya, T., Liu, D., Sun, M., 2011. Detrital and xenocrystic zircon ages from Neoproterozoic to Paleozoic arc terranes of Mongolia: significance for the origin of crustal fragments in the Central Asian Orogenic Belt. Gondwana Research 19, 751–763.
Rudnev, S.N., Vladimirov, A.G., Ponomarchuk, V.A., Kruk, N.N., Babin, G.A., Borisov, S.M., 2004. Early Paleozoic granitoid batholiths of the Altai-Sayan folded region (lateral–temporal zoning and sources). Doklady Earth Sciences 396, 492–495 (In Russian).
Rudnev, S.N., Borisov, S.M., Babin, G.A., Levchenkov, O.A., Makeev, A.F., Serov, P.A., Matukov, D.I., Plotkina, Y.V., 2008. Early Paleozoic batholiths in the northern part of the Kuznetsk Alatau: composition, age, and sources. Petrology 16, 395–419.
Safonova, I.Y., Buslov, M.M., Iwata, K., Kokh, D.A., 2004. Fragments of Vendian–early Carboniferous oceanic crust of the Paleo-Asian Ocean in foldbelts of the Altai-Sayan region of Central Asia: geochemistry, biostratigraphy and structural setting. Gondwana Research 7, 771–790.
Safonova, I.Y., Simonov, V.A., Buslov, M.M., Ota, T., Maruyama, S., 2008. Neoproterozoic basalts of the Paleo-Asian Ocean (Kurai accretionary zone, Gorny Altai, Russia): geochemistry, petrogenesis, and geodynamics. Russian Geology and Geophysics 49, 254–271.
Safonova, I.Y., Utsunomiya, A., Kojima, S., Nakae, S., Tomurtogoo, O., Filippov, A.N., Koizumi, K., 2009. Pacific superplume-related oceanic basalts hosted by accretionary complexes of Central Asia, Russian Far East and Japan. Gondwana Research 16, 587–608.
Safonova, I.Y., Maruyama, S., Hirata, T., Kon, Y., Rino, S., 2010. LA ICP MS U–Pb ages of detrital zircons from Russia largest rivers: implications for major granitoid events in Eurasia and global episodes of supercontinent formation. Journal of Geodynamics 50, 134–153.
Şengör, A.M.C., Natalin, B.A., Burtman, V.S., 1993. Evolution of the Altaid tectonic collage and Paleozoic crustal growth in Eurasia. Nature 364, 299–307.
Sennikov, N.V., Kazansky, A.Y., Iwata, K., Obut, O.T., Sugai, Y., Zybin, V.A., Khlebnikova, T.V., 2004. Comparative position of Bateny and Biya-Katun' terrains (Altai-Sayan Folded Area, Russia) in the Cambrian based on combined paleomagnetic, lithologic and paleontological data. Gondwana Research 7, 833–841.
Sláma, J., Kosler, J., Condon, D.J., Crowley, J.L., Gerdes, A., Hanchar, J.M., Horstwood, M.S.A., Morris, G.A., Nasdala, L., Norberg, N., Schaltegger, U., Schoene, B., Tubrett, M.N., Whitehouse, M.J., 2008. Plešovice zircon — a new natural reference material for U–Pb and Hf isotopic microanalysis. Chemical Geology 249, 1–35.
Stacey, J.S., Kramers, J.D., 1975. Approximation of terrestrial lead isotope evolution by a 2-stage model. Earth and Planetary Science Letters 26, 207–221.
Sun, M., Yuan, C., Xiao, W., Long, X., Xia, X., Zhao, G., Lin, S., Wu, F., Kroner, A., 2008. Zircon U–Pb and Hf isotopic study of gneissic rocks from the Chinese Altai: progressive accretionary history in the early to middle Palaeozoic. Chemical Geology 247, 352–383.
Uchio, Y., Isozaki, Y., Buslov, M.M., Maruyama, S., 2008. Occurrence of phosphatic microfossils in an Ediacaran–Cambrian mid-oceanic paleo-atoll limestone of southern Siberia. Gondwana Research 14, 183–192.
Utsunomiya, A., Jahn, B., Ota, T., Safonova, I.Y., 2009. A geochemical and Sr–Nd isotopic study of the Vendian greenstones from Gorny Altai, southern Siberia: implications for the tectonic setting of the formation of greenstones and the role of oceanic plateaus in accretionary orogen. Lithos 113, 437–453.
Vladimirov, A.G., Kozlov, M.S., Shokal'skii, S.P., Khalilov, V.A., Rudnev, S.N., Kruk, N.N., Vystavnoi, S.A., Borisov, S.M., Berezikov, Y.K., Metsner, A.N., Babin, G.A., Mamlin, A.N., Murzin, O.M., Nazarov, G.V., Makarov, V.A., 2001. Major epochs of instrusive magmatism of Kuznetsk Alatau, Altai, and Kalba (from U–Pb isotope dates). Russian Geology and Geophysics 42, 1157–1178.
Volkova, N.I., Sklyarov, E.V., 2007. High-pressure complexes of Central Asian Fold Belt: geologic setting, geochemistry, and geodynamic implications. Russian Geology and Geophysics 48, 83–90.
Volkova, N.I., Stupakov, S.I., Tret'yakov, G.A., Simonov, V.A., Travin, A.V., Yudin, D.S., 2005. Blueschists from the Uimon Zone as evidence for Ordovician accretionary-collisional events in Gorny Altai. Russian Geology and Geophysics 46, 361–378.
Wang, T., Hong, D.W., Jahn, B.M., Tong, Y., Wang, Y.B., Han, B.F., Wang, X.X., 2006. Timing, petrogenesis, and setting of Paleozoic synorogenic intrusions from the Altai Mountains, northwest China: implications for the tectonic evolution of an accretionary orogen. Journal of Geology 114, 735–751.
Wang, T., Jahn, B.M., Kovach, V.P., Tong, Y., Hong, D.W., Han, B.F., 2009. Nd–Sr isotopic mapping of the Chinese Altai and implications for continental growth in the Central Asian Orogenic Belt. Lithos 110, 359–372.
Windley, B.F., Kröner, A., Guo, J.H., Qu, G.S., Li, Y.Y., Zhang, C., 2002. Neoproterozoic to Paleozoic geology of the Altai orogen, NW China: new zircon age data and tectonic evolution. Journal of Geology 110, 719–737.
Windley, B.F., Alexeiev, D., Xiao, W.J., Kroner, A., Badarch, G., 2007. Tectonic models for accretion of the Central Asian Orogenic Belt. Journal of the Geological Society of London 164, 31–47.
Wu, F.Y., Sun, D.Y., Li, H.M., Jahn, B.M., Wilde, S., 2002. A-type granites in northeastern China: age and geochemical constraints on their petrogenesis. Chemical Geology 187, 143–173.
Xiao, W., Windley, B.F., Badarch, G., Sun, S., Li, J., Qin, K., Wang, Z., 2004. Palaeozoic accretionary and convergent tectonics of the southern Altaids: implications for the growth of Central Asia. Journal of the Geological Society 161, 339–342.
Xiao, W.J., Windley, B.F., Yuan, C., Sun, M., Han, C.M., Lin, S.F., Chen, H.L., Yan, Q.R., Liu, D.Y., Qin, K.Z., Li, J.L., Sun, S., 2009. Paleozoic multiple subduction–accretion processes of the southern Altaids. American Journal of Science 309, 221–270.
Yamamoto, S., Senshu, H., Rino, S., Omori, S., Maruyama, S., 2009. Granite subduction: arc subduction, tectonic erosion and sediment subduction. Gondwana Research 15, 443–453.
Yuan, C., Sun, M., Xiao, W., Li, X., Chen, H., Lin, S., Xia, X., Long, X., 2007. Accretionary orogenesis of the Chinese Altai: insights from Paleozoic granitoids. Chemical Geology 242, 22–39.
Yuan, C., Sun, M., Wilde, S., Xiao, W.J., Xu, Y.G., Long, X.P., Zhao, G.C., 2010. Post-collisional plutons in the Balikun area, East Chinese Tianshan: evolving magmatism in response to extension and slab break-off. Lithos 119, 269–288.
Zhao, G.C., Cawood, P.A., Wilde, S.A., Sun, M., 2002. Review of global 2.1–1.8 Ga orogens: implications for a pre-Rodinia supercontinent. Earth-Science Reviews 59, 125–162.
Zhao, G.C., Sun, M., Wilde, S.A., Li, S.Z., Zhang, J., 2006. Some key issues in reconstructions of Proterozoic supercontinents. Journal of Asian Earth Sciences 28, 3–19.